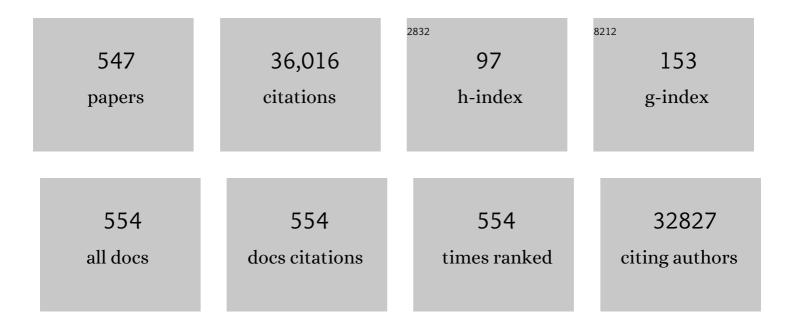
Jiuhui Qu

List of Publications by Year in descending order

Source: https://exaly.com/author-pdf/2001241/publications.pdf Version: 2024-02-01



| # | Article | IF | CITATIONS |
|----|---|-----|-----------|
| 1 | Removal of pharmaceutical in a biogenic/chemical manganese oxide system driven by manganese-oxidizing bacteria with humic acids as sole carbon source. Journal of Environmental Sciences, 2023, 126, 734-741. | 3.2 | 14 |
| 2 | The Phragmites Root-Inhabiting Microbiome: A Critical Review on Its Composition and Environmental Application. Engineering, 2022, 9, 42-50. | 3.2 | 14 |
| 3 | Impact of microplastics on the foraging, photosynthesis and digestive systems of submerged carnivorous macrophytes under low and high nutrient concentrations. Environmental Pollution, 2022, 292, 118220. | 3.7 | 31 |
| 4 | Environmental heterogeneity determines the response patterns of microbially mediated N-reduction processes to sulfamethoxazole in river sediments. Journal of Hazardous Materials, 2022, 421, 126730. | 6.5 | 16 |
| 5 | Mixing regime shapes the community assembly process, microbial interaction and proliferation of cyanobacterial species Planktothrix in a stratified lake. Journal of Environmental Sciences, 2022, 115, 103-113. | 3.2 | 7 |
| 6 | Profiling microbial removal of micropollutants in sand filters: Biotransformation pathways and associated bacteria. Journal of Hazardous Materials, 2022, 423, 127167. | 6.5 | 14 |
| 7 | Can radicals-orientated chemical oxidation improve the reduction of antibiotic resistance genes (ARGs) by mesophilic anaerobic digestion of sludge?. Journal of Hazardous Materials, 2022, 426, 128001. | 6.5 | 12 |
| 8 | Siderophores provoke extracellular superoxide production by <i>Arthrobacter</i> strains during carbon sourcesâ€level fluctuation. Environmental Microbiology, 2022, 24, 894-904. | 1.8 | 5 |
| 9 | Red mud supported on reduced graphene oxide as photo-Fenton catalysts for organic contaminant degradation. Colloids and Surfaces A: Physicochemical and Engineering Aspects, 2022, 640, 128461. | 2.3 | 9 |
| 10 | Characterization on the formation mechanism of Fe0/Fe3C/C nanostructure and its effect on PMS activation performance towards BPA degradation. Chemical Engineering Journal, 2022, 435, 134709. | 6.6 | 3 |
| 11 | Persistence of SARS-CoV-2 RNA in wastewater after the end of the COVID-19 epidemics. Journal of Hazardous Materials, 2022, 429, 128358. | 6.5 | 38 |
| 12 | Insight into the Key Role of Cr Intermediates in the Efficient and Simultaneous Degradation of Organic Contaminants and Cr(VI) Reduction via g-C ₃ N ₄ -Assisted Photocatalysis. Environmental Science & Technology, 2022, 56, 3552-3563. | 4.6 | 48 |
| 13 | Simultaneous Phenol Removal and Resource Recovery from Phenolic Wastewater by Electrocatalytic Hydrogenation. Environmental Science & Technology, 2022, 56, 4356-4366. | 4.6 | 43 |
| 14 | Simultaneous removal of aromatic pollutants and nitrate at high concentrations by hypersaline denitrification:Long-term continuous experiments investigation. Water Research, 2022, 216, 118292. | 5.3 | 16 |
| 15 | Oxygenated polycyclic aromatic hydrocarbons in the surface water environment: Occurrence, ecotoxicity, and sources. Environment International, 2022, 163, 107232. | 4.8 | 22 |
| 16 | Polyethylene microplastics interfere with the nutrient cycle in water-plant-sediment systems. Water Research, 2022, 214, 118191. | 5.3 | 40 |
| 17 | The biogeochemical responses of hyporheic groundwater to the long-run managed aquifer recharge: Linking microbial communities to hydrochemistry and micropollutants. Journal of Hazardous Materials, 2022, 431, 128587. | 6.5 | 16 |
| 18 | A homogeneous reagent for Ni2+ capture from wastewater: The phase transition mechanism and impact evaluation for aerobic sludge. Chemical Engineering Journal, 2022, 440, 135809. | 6.6 | 1 |

| # | Article | IF | CITATIONS |
|----|--|------|-----------|
| 19 | Do NH4+-N and AOB affect atenolol removal during simulated riverbank filtration?. Chemosphere, 2022, 301, 134653. | 4.2 | 2 |
| 20 | Synergy of cyano groups and cobalt single atoms in graphitic carbon nitride for enhanced bio-denitrification. Water Research, 2022, 218, 118465. | 5.3 | 19 |
| 21 | Spatiotemporal variation and risk assessment of phthalate acid esters (PAEs) in surface water of the Yangtze River Basin, China. Science of the Total Environment, 2022, 836, 155677. | 3.9 | 23 |
| 22 | Long-term direct ultrafiltration without chemical cleaning for purification of micro-polluted water in rural regions: Feasibility and application prospects. Chemical Engineering Journal, 2022, 443, 136531. | 6.6 | 3 |
| 23 | Synchronous Moderate Oxidation and Adsorption on the Surface of Î ³ -MnO ₂ for Efficient Iodide Removal from Water. Environmental Science & Technology, 2022, 56, 9417-9427. | 4.6 | 10 |
| 24 | Visualization of Electrochemically Accessible Sites in Flow-through Mode for Maximizing Available Active Area toward Superior Electrocatalytic Ammonia Oxidation. Environmental Science & Technology, 2022, 56, 9722-9731. | 4.6 | 15 |
| 25 | Interface-modulated nanojunction and microfluidic platform for photoelectrocatalytic chemicals upgrading. Applied Catalysis B: Environmental, 2021, 282, 119541. | 10.8 | 29 |
| 26 | Growth inhibition of Microcystis aeruginosa by sand-filter prevalent manganese-oxidizing bacterium. Separation and Purification Technology, 2021, 256, 117808. | 3.9 | 4 |
| 27 | Selection of water source for water transfer based on algal growth potential to prevent algal blooms. Journal of Environmental Sciences, 2021, 103, 246-254. | 3.2 | 7 |
| 28 | Hotâ€Electronâ€Induced Photothermal Catalysis for Energyâ€Dependent Molecular Oxygen Activation. Angewandte Chemie, 2021, 133, 4922-4928. | 1.6 | 9 |
| 29 | Synergistic effect of dual sites on bimetal-organic frameworks for highly efficient peroxide activation. Journal of Hazardous Materials, 2021, 406, 124692. | 6.5 | 52 |
| 30 | Epilithic biofilm as a reservoir for functional virulence factors in wastewater-dominant rivers after WWTP upgrade. Journal of Environmental Sciences, 2021, 101, 27-35. | 3.2 | 13 |
| 31 | Parent and Substitute Polycyclic Aromatic Hydrocarbon Reduction in Urban Rivers—Benefits of the Energy Transition Policy from 2009 to 2017 in Beijing, China. ACS ES&T Water, 2021, 1, 815-824. | 2.3 | 2 |
| 32 | Revealing Surface Charge Population on Flake-Like BiVO ₄ Photocatalysts by Single Particle Imaging Spectroscopies. ACS Applied Energy Materials, 2021, 4, 2543-2551. | 2.5 | 16 |
| 33 | Synergetic Hydroxyl Radical Oxidation with Atomic Hydrogen Reduction Lowers the Organochlorine Conversion Barrier and Potentiates Effective Contaminant Mineralization. Environmental Science & Technology, 2021, 55, 3296-3304. | 4.6 | 39 |
| 34 | Synergetic Lipid Extraction with Oxidative Damage Amplifies Cellâ€Membraneâ€Destructive Stresses and Enables Rapid Sterilization. Angewandte Chemie - International Edition, 2021, 60, 7744-7751. | 7.2 | 26 |
| 35 | Synergetic Lipid Extraction with Oxidative Damage Amplifies Cellâ€Membraneâ€Destructive Stresses and Enables Rapid Sterilization. Angewandte Chemie, 2021, 133, 7823-7830. | 1.6 | 10 |
| 36 | Three-Dimensional Analysis of the Natural-Organic-Matter Distribution in the Cake Layer to Precisely Reveal Ultrafiltration Fouling Mechanisms. Environmental Science & Technology, 2021, 55, 5442-5452. | 4.6 | 38 |

| # | Article | IF | CITATIONS |
|----|--|------|-----------|
| 37 | Regulating Oriented Adsorption on Targeted Nickel Sites for Antibiotic Oxidation with Simultaneous Hydrogen Energy Recovery by a Direct Electrochemical Process. ACS Applied Materials & Interfaces, 2021, 13, 18673-18682. | 4.0 | 11 |
| 38 | â€~Blue Route' for combating climate change. National Science Review, 2021, 8, nwab099. | 4.6 | 2 |
| 39 | Electricity generation from salinity gradient to remove chromium using reverse electrodialysis coupled with electrocoagulation. Electrochimica Acta, 2021, 379, 138153. | 2.6 | 13 |
| 40 | U.S.–China Collaboration is Vital to Clobal Plans for a Healthy Environment and Sustainable Development. Environmental Science & Technology, 2021, 55, 9622-9626. | 4.6 | 10 |
| 41 | Spatial variation of dissolved organic nitrogen in Wuhan surface waters: Correlation with the occurrence of disinfection byproducts during the COVID-19 pandemic. Water Research, 2021, 198, 117138. | 5.3 | 27 |
| 42 | Emerging graphitic carbon nitride-based membranes for water purification. Water Research, 2021, 200, 117207. | 5.3 | 53 |
| 43 | Ultra-fast and onsite interrogation of Severe Acute Respiratory Syndrome Coronavirus 2 (SARS-CoV-2) in waters via surface enhanced Raman scattering (SERS). Water Research, 2021, 200, 117243. | 5.3 | 77 |
| 44 | Removal of p-arsanilic acid and phenylarsonic acid from water by Fenton coagulation process: influence of substituted amino group. Environmental Science and Pollution Research, 2021, 28, 63319-63329. | 2.7 | 3 |
| 45 | Machine learning approach identifies water sample source based on microbial abundance. Water Research, 2021, 199, 117185. | 5.3 | 18 |
| 46 | <i>In Situ</i> Characterization of Dehydration during Ion Transport in Polymeric Nanochannels. Journal of the American Chemical Society, 2021, 143, 14242-14252. | 6.6 | 89 |
| 47 | Recovery trajectories and community resilience of biofilms in receiving rivers after wastewater treatment plant upgrade. Environmental Research, 2021, 199, 111349. | 3.7 | 10 |
| 48 | Transformation of typical components in anaerobically digested sludge during its conditioning process by KMnO4. Resources, Conservation and Recycling, 2021, 171, 105657. | 5.3 | 13 |
| 49 | Optimization of a Hierarchical Porous-Structured Reactor to Mitigate Mass Transport Limitations for Efficient Electrocatalytic Ammonia Oxidation through a Three-Electron-Transfer Pathway. Environmental Science & Technology, 2021, 55, 12596-12606. | 4.6 | 24 |
| 50 | Manganese oxides in Phragmites rhizosphere accelerates ammonia oxidation in constructed wetlands. Water Research, 2021, 205, 117688. | 5.3 | 32 |
| 51 | Microplastic residues in wetland ecosystems: Do they truly threaten the plant-microbe-soil system?. Environment International, 2021, 156, 106708. | 4.8 | 115 |
| 52 | SARS-CoV-2 spillover into hospital outdoor environments. Journal of Hazardous Materials Letters, 2021, 2, 100027. | 2.0 | 33 |
| 53 | A dual-biomimetic photocatalytic fuel cell for efficient electricity generation from degradation of refractory organic pollutants. Applied Catalysis B: Environmental, 2021, 298, 120501. | 10.8 | 26 |
| 54 | Review on heterogeneous oxidation and adsorption for arsenic removal from drinking water. Journal of Environmental Sciences, 2021, 110, 178-188. | 3.2 | 41 |

| # | Article | IF | CITATIONS |
|----|--|------|-----------|
| 55 | Insight into electroreductive activation process of peroxydisulfate for eliminating organic pollution: Essential role of atomic hydrogen. Chemical Engineering Journal, 2021, 426, 128355. | 6.6 | 18 |
| 56 | Pre-oxidation enhanced cyanobacteria removal in drinking water treatment: A review. Journal of Environmental Sciences, 2021, 110, 160-168. | 3.2 | 30 |
| 57 | Roadmap for Managing SARS-CoV-2 and other Viruses in the Water Environment for Public Health. Engineering, 2021, , . | 3.2 | 6 |
| 58 | In Situ Creation of Oxygen Vacancies in Porous Bimetallic La/Zr Sorbent for Aqueous Phosphate: Hierarchical Pores Control Mass Transport and Vacancy Sites Determine Interaction. Environmental Science & Technology, 2020, 54, 437-445. | 4.6 | 34 |
| 59 | Identification and quantification of bacterial genomes carrying antibiotic resistance genes and virulence factor genes for aquatic microbiological risk assessment. Water Research, 2020, 168, 115160. | 5.3 | 102 |
| 60 | Regioselective oxidation of tetracycline by permanganate through alternating susceptible moiety and increasing electron donating ability. Journal of Environmental Sciences, 2020, 87, 281-288. | 3.2 | 17 |
| 61 | Polyoxometalates/TiO2 photocatalysts with engineered facets for enhanced degradation of bisphenol A through persulfate activation. Applied Catalysis B: Environmental, 2020, 268, 118394. | 10.8 | 88 |
| 62 | Assessing food web health with network topology and stability analysis in aquatic ecosystem. Ecological Indicators, 2020, 109, 105820. | 2.6 | 3 |
| 63 | Enhanced phosphate removal using zirconium hydroxide encapsulated in quaternized cellulose. Journal of Environmental Sciences, 2020, 89, 102-112. | 3.2 | 32 |
| 64 | Efficient Microcystis aeruginosa removal by moderate photocatalysis-enhanced coagulation with magnetic Zn-doped Fe3O4 particles. Water Research, 2020, 171, 115448. | 5.3 | 85 |
| 65 | Recyclable Printed Circuit Boards and Alkali Reduction Wastewater: Approach to a Sustainable Copper-Based Metal–Organic Framework. ACS Sustainable Chemistry and Engineering, 2020, 8, 1371-1379. | 3.2 | 21 |
| 66 | Low electronegativity Mn bulk doping intensifies charge storage of Ni ₂ P redox shuttle for membrane-free water electrolysis. Journal of Materials Chemistry A, 2020, 8, 4073-4082. | 5.2 | 26 |
| 67 | Influence of sedimentation with pre-coagulation on ultrafiltration membrane fouling performance. Science of the Total Environment, 2020, 708, 134671. | 3.9 | 14 |
| 68 | Influence of floc dynamic protection layer on alleviating ultrafiltration membrane fouling induced by humic substances. Journal of Environmental Sciences, 2020, 90, 10-19. | 3.2 | 4 |
| 69 | Enhanced alleviation of ultrafiltration membrane fouling by regulating cake layer thickness with pre-coagulation during drinking water treatment. Journal of Membrane Science, 2020, 596, 117732. | 4.1 | 29 |
| 70 | New insights into the surface-dependent activity of graphitic felts for the electro-generation of H2O2. Applied Surface Science, 2020, 509, 144875. | 3.1 | 25 |
| 71 | Denitrification enhancement by electro-sorption/reduction using a layered metal oxide electrode loaded with Pd-Cu nanoparticles. Electrochemistry Communications, 2020, 110, 106607. | 2.3 | 11 |
| 72 | Isotopic and chemical evidence for nitrate sources and transformation processes in a plateau lake basin in Southwest China. Science of the Total Environment, 2020, 711, 134856. | 3.9 | 30 |

| # | Article | IF | CITATIONS |
|----|---|------|-----------|
| 73 | Visualizing the Interfacial Charge Transfer between Photoactive <i>Microcystis aeruginosa</i> and Hydrogenated TiO ₂ . Environmental Science & Technology, 2020, 54, 10323-10332. | 4.6 | 21 |
| 74 | Effects of a spatially heterogeneous nutrient distribution on the growth of clonal wetland plants. BMC Ecology, 2020, 20, 59. | 3.0 | 14 |
| 75 | Survey-based approach to establish macrobenthic biological network in lakes. Resources, Conservation and Recycling, 2020, 162, 105061. | 5.3 | 0 |
| 76 | Arrayed Cobalt Phosphide Electrocatalyst Achieves Low Energy Consumption and Persistent H2 Liberation from Anodic Chemical Conversion. Nano-Micro Letters, 2020, 12, 154. | 14.4 | 29 |
| 77 | pH-Independent Production of Hydroxyl Radical from Atomic H*-Mediated Electrocatalytic H ₂ O ₂ Reduction: A Green Fenton Process without Byproducts. Environmental Science & Technology, 2020, 54, 14725-14731. | 4.6 | 106 |
| 78 | Carbon harvesting from organic liquid wastes for heterotrophic denitrification: Feasibility evaluation and cost and emergy optimization. Resources, Conservation and Recycling, 2020, 160, 104782. | 5.3 | 9 |
| 79 | A salt-rejecting anisotropic structure for efficient solar desalination <i>via</i> heat–mass flux decoupling. Journal of Materials Chemistry A, 2020, 8, 12089-12096. | 5.2 | 27 |
| 80 | Electrochemical-Osmotic Process for Simultaneous Recovery of Electric Energy, Water, and Metals from Wastewater. Environmental Science & Technology, 2020, 54, 8430-8442. | 4.6 | 31 |
| 81 | One-step exfoliation of polymeric C3N4 by atmospheric oxygen doping for photocatalytic persulfate activation. Journal of Colloid and Interface Science, 2020, 579, 455-462. | 5.0 | 28 |
| 82 | Sedimentary ancient DNA metabarcoding delineates the contrastingly temporal change of lake cyanobacterial communities. Water Research, 2020, 183, 116077. | 5.3 | 22 |
| 83 | Enhancement of anti-fouling and contaminant removal in an electro-membrane bioreactor: Significance of electrocoagulation and electric field. Separation and Purification Technology, 2020, 248, 117077. | 3.9 | 40 |
| 84 | Ultrathin water-stable metal-organic framework membranes for ion separation. Science Advances, 2020, 6, eaay3998. | 4.7 | 179 |
| 85 | Dual channel construction of WO3 photocatalysts by solution plasma for the persulfate-enhanced photodegradation of bisphenol A. Applied Catalysis B: Environmental, 2020, 277, 119221. | 10.8 | 56 |
| 86 | Ecotoxicity of polystyrene microplastics to submerged carnivorous Utricularia vulgaris plants in freshwater ecosystems. Environmental Pollution, 2020, 265, 114830. | 3.7 | 69 |
| 87 | Hierarchically porous UiO-66 with tunable mesopores and oxygen vacancies for enhanced arsenic removal. Journal of Materials Chemistry A, 2020, 8, 7870-7879. | 5.2 | 132 |
| 88 | Graphitic N in nitrogen-Doped carbon promotes hydrogen peroxide synthesis from electrocatalytic oxygen reduction. Carbon, 2020, 163, 154-161. | 5.4 | 131 |
| 89 | Metagenomics Unravels Differential Microbiome Composition and Metabolic Potential in Rapid Sand Filters Purifying Surface Water Versus Groundwater. Environmental Science & Technology, 2020, 54, 5197-5206. | 4.6 | 51 |
| 90 | Potassium-Ion Recovery with a Polypyrrole Membrane Electrode in Novel Redox Transistor Electrodialysis. Environmental Science & Technology, 2020, 54, 4592-4600. | 4.6 | 17 |

| # | Article | IF | CITATIONS |
|-----|--|------|-----------|
| 91 | Potential spreading risks and disinfection challenges of medical wastewater by the presence of Severe Acute Respiratory Syndrome Coronavirus 2 (SARS-CoV-2) viral RNA in septic tanks of Fangcang Hospital. Science of the Total Environment, 2020, 741, 140445. | 3.9 | 236 |
| 92 | Influence of floc charge and related distribution mechanisms of humic substances on ultrafiltration membrane behavior. Journal of Membrane Science, 2020, 609, 118260. | 4.1 | 8 |
| 93 | Effects of 1-hydroxyethane-(1,1-bisphosphonic acid) on heterotrophic denitrification performance: Impact of denitrifying microbial communities variation. Chemical Engineering Journal, 2020, 402, 126210. | 6.6 | 9 |
| 94 | Defect-enhanced photocatalytic removal of dimethylarsinic acid over mixed-phase mesoporous TiO2. Journal of Environmental Sciences, 2020, 91, 35-42. | 3.2 | 15 |
| 95 | Zinc Substitutionâ€Induced Subtle Lattice Distortion Mediates the Active Center of Cobalt Diselenide Electrocatalysts for Enhanced Oxygen Evolution. Small, 2020, 16, e1907001. | 5.2 | 37 |
| 96 | Manipulation of Neighboring Palladium and Mercury Atoms for Efficient *OH Transformation in Anodic Alcohol Oxidation and Cathodic Oxygen Reduction Reactions. ACS Applied Materials & Interfaces, 2020, 12, 12677-12685. | 4.0 | 12 |
| 97 | A layered aluminum-based metal–organic framework as a superior trap for nitrobenzene capture via an intercalation role. Nanoscale, 2020, 12, 6012-6019. | 2.8 | 6 |
| 98 | Anaerobically-digested sludge disintegration by transition metal ions-activated peroxymonosulfate (PMS): Comparison between Co2+, Cu2+, Fe2+ and Mn2+. Science of the Total Environment, 2020, 713, 136530. | 3.9 | 80 |
| 99 | Carbon nanodot-modified FeOCl for photo-assisted Fenton reaction featuring synergistic in-situ H2O2 production and activation. Applied Catalysis B: Environmental, 2020, 266, 118665. | 10.8 | 108 |
| 100 | Wastewater treatment plant upgrade induces the receiving river retaining bioavailable nitrogen sources. Environmental Pollution, 2020, 263, 114478. | 3.7 | 21 |
| 101 | Improving ion rejection of graphene oxide conductive membranes by applying electric field. Journal of Membrane Science, 2020, 604, 118077. | 4.1 | 17 |
| 102 | Reversible superwettability switching of a conductive polymer membrane for oil-water separation and self-cleaning. Journal of Membrane Science, 2020, 605, 118088. | 4.1 | 30 |
| 103 | Mechanism of species dynamics and interactions under impacts of artificial barriers in coastal areas. Ocean and Coastal Management, 2020, 190, 105166. | 2.0 | 3 |
| 104 | Microbial community structures and functions of hypersaline heterotrophic denitrifying process: Lab-scale and pilot-scale studies. Bioresource Technology, 2020, 310, 123244. | 4.8 | 26 |
| 105 | Development of Amyloid-Fibrils-like Functional Materials from Both Anaerobically Digested Sludge and Waste Activated Sludge for Heavy Metal Adsorption. ACS Sustainable Chemistry and Engineering, 2020, 8, 7795-7805. | 3.2 | 13 |
| 106 | Fouling mitigation of a graphene hydrogel membrane electrode by electrical repulsion and in situ self-cleaning in an electro-membrane reactor. Chemical Engineering Journal, 2020, 393, 124817. | 6.6 | 32 |
| 107 | Effects of resource heterogeneity and environmental disturbance on the growth performance and interspecific competition of wetland clonal plants. Global Ecology and Conservation, 2020, 22, e00914. | 1.0 | 10 |
| 108 | A promising treatment method for Cr(VI) detoxification and recovery by coupling Fe0/Fe3C/C fine powders and circulating fluidized bed. Chemical Engineering Journal, 2020, 398, 125565. | 6.6 | 8 |

| # | Article | IF | CITATIONS |
|-----|---|-----|-----------|
| 109 | Preferential binding between intracellular organic matters and Al13 polymer to enhance coagulation performance. Journal of Environmental Sciences, 2019, 76, 1-11. | 3.2 | 17 |
| 110 | Micro-electrode system designed to determine H+ concentration distribution at particle-water interface. Science of the Total Environment, 2019, 646, 544-550. | 3.9 | 4 |
| 111 | Interfacial Engineering of SeO Ligands on Tellurium Featuring Synergistic Functionalities of Bond Activation and Chemical States Buffering toward Electrocatalytic Conversion of Nitrogen to Ammonia. Advanced Science, 2019, 6, 1901627. | 5.6 | 32 |
| 112 | Effect of pre-coagulation using different aluminium species on crystallization of cake layer and membrane fouling. Npj Clean Water, 2019, 2, . | 3.1 | 7 |
| 113 | Electrically Poreâ€Sizeâ€Tunable Polypyrrole Membrane for Antifouling and Selective Separation. Advanced Functional Materials, 2019, 29, 1903081. | 7.8 | 45 |
| 114 | Combining KMnO4 pre-oxidation and bioaugmented sand filtration to simultaneously treat cyanobacterial bloom lake water and released Mn(II). Separation and Purification Technology, 2019, 228, 115765. | 3.9 | 11 |
| 115 | Defect Modulation of Z-Scheme TiO ₂ /Cu ₂ O Photocatalysts for Durable Water Splitting. ACS Catalysis, 2019, 9, 8346-8354. | 5.5 | 146 |
| 116 | Triggering of Low-Valence Molybdenum in Multiphasic MoS ₂ for Effective Reactive Oxygen Species Output in Catalytic Fenton-like Reactions. ACS Applied Materials & Interfaces, 2019, 11, 26781-26788. | 4.0 | 76 |
| 117 | Spatial distribution of flow currents and habitats in artificial buffer zones for ecosystem-based coastal engineering. Global Ecology and Conservation, 2019, 20, e00764. | 1.0 | 2 |
| 118 | Synergetic Photocatalytic Pure Water Splitting and Self-Supplied Oxygen Activation by 2-D WO ₃ /TiO ₂ Heterostructures. ACS Sustainable Chemistry and Engineering, 2019, 7, 19902-19909. | 3.2 | 18 |
| 119 | Enhanced Stabilization and Effective Utilization of Atomic Hydrogen on Pd–In Nanoparticles in a Flow-through Electrode. Environmental Science & Technology, 2019, 53, 11383-11390. | 4.6 | 60 |
| 120 | Modulation of cation trans-membrane transport in GO-MoS2 membranes through simultaneous control of interlayer spacing and ion-nanochannel interactions. Chemosphere, 2019, 222, 156-164. | 4.2 | 22 |
| 121 | Application of Integrated Bioelectrochemical-Wetland Systems for Future Sustainable Wastewater Treatment. Environmental Science & Technology, 2019, 53, 1741-1743. | 4.6 | 33 |
| 122 | Tracking Internal Electron Shuttle Using X-ray Spectroscopies in La/Zr Hydroxide for Reconciliation of Charge-Transfer Interaction and Coordination toward Phosphate. ACS Applied Materials & Interfaces, 2019, 11, 24699-24706. | 4.0 | 22 |
| 123 | Engineering Carbon Nanotube Forest Superstructure for Robust Thermal Desalination Membranes. Advanced Functional Materials, 2019, 29, 1903125. | 7.8 | 48 |
| 124 | Faceted TiO2 photocatalytic degradation of anthraquinone in aquatic solution under solar irradiation. Science of the Total Environment, 2019, 688, 592-599. | 3.9 | 29 |
| 125 | Activation of Lattice Oxygen in LaFe (Oxy)hydroxides for Efficient Phosphorus Removal. Environmental Science & Technology, 2019, 53, 9073-9080. | 4.6 | 94 |
| 126 | Hydrogen-Bond-Mediated Self-Assembly of Carbon-Nitride-Based Photo-Fenton-like Membranes for Wastewater Treatment. Environmental Science & Technology, 2019, 53, 6981-6988. | 4.6 | 79 |

| # | Article | IF | CITATIONS |
|-----|---|------|-----------|
| 127 | Anaerobically-digested sludge conditioning by activated peroxymonosulfate: Significance of EDTA chelated-Fe2+. Water Research, 2019, 160, 454-465. | 5.3 | 64 |
| 128 | Confining Free Radicals in Close Vicinity to Contaminants Enables Ultrafast Fentonâ€like Processes in the Interspacing of MoS ₂ Membranes. Angewandte Chemie - International Edition, 2019, 58, 8134-8138. | 7.2 | 419 |
| 129 | Membrane fouling reduction through electrochemically regulating flocs aggregation in an electro-coagulation membrane reactor. Journal of Environmental Sciences, 2019, 83, 144-151. | 3.2 | 24 |
| 130 | Confining Free Radicals in Close Vicinity to Contaminants Enables Ultrafast Fentonâ€like Processes in the Interspacing of MoS ₂ Membranes. Angewandte Chemie, 2019, 131, 8218-8222. | 1.6 | 23 |
| 131 | Enhanced Production of in Situ Keggin Al ₁₃ ⁷⁺ Polymer by a Combined Fe-Al Coagulation Process for the Treatment of High Alkalinity Water. ACS Sustainable Chemistry and Engineering, 2019, 7, 9544-9552. | 3.2 | 7 |
| 132 | The variation of flocs activity during floc breakage and aging, adsorbing phosphate, humic acid and clay particles. Water Research, 2019, 155, 131-141. | 5.3 | 57 |
| 133 | Intercalation of Nanosized Fe ₃ C in Iron/Carbon To Construct Multifunctional Interface with Reduction, Catalysis, Corrosion Resistance, and Immobilization Capabilities. ACS Applied Materials & Interfaces, 2019, 11, 15709-15717. | 4.0 | 50 |
| 134 | Field-Enhanced Nanoconvection Accelerated Electrocatalytic Conversion of Water Contaminants and Electricity Generation. Environmental Science & amp; Technology, 2019, 53, 2713-2719. | 4.6 | 12 |
| 135 | Triggering surface oxygen vacancies on atomic layered molybdenum dioxide for a low energy consumption path toward nitrogen fixation. Nano Energy, 2019, 59, 10-16. | 8.2 | 176 |
| 136 | Capillary-Flow-Optimized Heat Localization Induced by an Air-Enclosed Three-Dimensional Hierarchical Network for Elevated Solar Evaporation. ACS Applied Materials & Interfaces, 2019, 11, 9974-9983. | 4.0 | 48 |
| 137 | Synchronous Reduction–Oxidation Process for Efficient Removal of Trichloroacetic Acid: H* Initiates Dechlorination and ·OH Is Responsible for Removal Efficiency. Environmental Science & Technology, 2019, 53, 14586-14594. | 4.6 | 45 |
| 138 | Municipal wastewater treatment in China: Development history and future perspectives. Frontiers of Environmental Science and Engineering, 2019, 13, 1. | 3.3 | 238 |
| 139 | The International Conference on the Evolution of China Urban Water Environment & Ecology, 2019. Frontiers of Environmental Science and Engineering, 2019, 13, 1. | 3.3 | 4 |
| 140 | Effects of protein properties on ultrafiltration membrane fouling performance in water treatment. Journal of Environmental Sciences, 2019, 77, 273-281. | 3.2 | 43 |
| 141 | Dechlorination of triclosan by enhanced atomic hydrogen-mediated electrochemical reduction: Kinetics, mechanism, and toxicity assessment. Applied Catalysis B: Environmental, 2019, 241, 120-129. | 10.8 | 109 |
| 142 | Microfluidic-enhanced 3-D photoanodes with free interfacial energy barrier for photoelectrochemical applications. Applied Catalysis B: Environmental, 2019, 244, 740-747. | 10.8 | 29 |
| 143 | NOM fouling resistance in response to electric field during electro-ultrafiltration: Significance of molecular polarity and weight. Journal of Colloid and Interface Science, 2019, 539, 11-18. | 5.0 | 22 |
| 144 | Enhanced Photoreduction of Chromium(VI) Intercalated Ion Exchange in BiOBr0.7510.25 Layers Structure by Bulk Charge Transfer. ACS Sustainable Chemistry and Engineering, 2019, 7, 2429-2436. | 3.2 | 20 |

| # | Article | IF | CITATIONS |
|-----|--|------|-----------|
| 145 | Surface charge and hydrophilicity improvement of graphene membranes via modification of pore surface oxygen-containing groups to enhance permeability and selectivity. Carbon, 2019, 145, 140-148. | 5.4 | 55 |
| 146 | Selective adsorption of fluoride from drinking water using NiAl-layered metal oxide film electrode. Journal of Colloid and Interface Science, 2019, 539, 146-151. | 5.0 | 64 |
| 147 | Use of convertible flow cells to simulate the impacts of anthropogenic activities on river biofilm bacterial communities. Science of the Total Environment, 2019, 653, 148-156. | 3.9 | 18 |
| 148 | Polyoxometalates/TiO2 Fenton-like photocatalysts with rearranged oxygen vacancies for enhanced synergetic degradation. Applied Catalysis B: Environmental, 2019, 244, 407-413. | 10.8 | 92 |
| 149 | Characteristics of microplastic removal via coagulation and ultrafiltration during drinking water treatment. Chemical Engineering Journal, 2019, 359, 159-167. | 6.6 | 382 |
| 150 | Removal characteristics of microplastics by Fe-based coagulants during drinking water treatment. Journal of Environmental Sciences, 2019, 78, 267-275. | 3.2 | 235 |
| 151 | Removal of micropollutants and cyanobacteria from drinking water using KMnO4 pre-oxidation coupled with bioaugmentation. Chemosphere, 2019, 215, 1-7. | 4.2 | 32 |
| 152 | Oxygen vacancy modulation of {010}-dominated TiO2 for enhanced photodegradation of Sulfamethoxazole. Catalysis Communications, 2019, 118, 35-38. | 1.6 | 13 |
| 153 | Reinventing Fenton Chemistry: Iron Oxychloride Nanosheet for pH-Insensitive H ₂ O ₂ Activation. Environmental Science and Technology Letters, 2018, 5, 186-191. | 3.9 | 202 |
| 154 | Electrochemical oxidation of ammonia accompanied with electricity generation based on reverse electrodialysis. Electrochimica Acta, 2018, 269, 128-135. | 2.6 | 32 |
| 155 | Integrating microbial biomass, composition and function to discern the level of anthropogenic activity in a river ecosystem. Environment International, 2018, 116, 147-155. | 4.8 | 78 |
| 156 | Multiple dynamic Al-based floc layers on ultrafiltration membrane surfaces for humic acid and reservoir water fouling reduction. Water Research, 2018, 139, 291-300. | 5.3 | 39 |
| 157 | The effects of hydrogen peroxide pre-oxidation on ultrafiltration membrane biofouling alleviation in drinking water treatment. Journal of Environmental Sciences, 2018, 73, 117-126. | 3.2 | 17 |
| 158 | Strongly Coupled Metal Oxide/Reassembled Carbon Nitride/Co–Pi Heterostructures for Efficient Photoelectrochemical Water Splitting. ACS Applied Materials & Interfaces, 2018, 10, 6424-6432. | 4.0 | 50 |
| 159 | Enhancement of the Donnan effect through capacitive ion increase using an electroconductive rGO-CNT nanofiltration membrane. Journal of Materials Chemistry A, 2018, 6, 4737-4745. | 5.2 | 82 |
| 160 | Benzophenone-4 Promotes the Growth of a <i>Pseudomonas</i> sp. and Biogenic Oxidation of Mn(II). Environmental Science & Technology, 2018, 52, 1262-1269. | 4.6 | 18 |
| 161 | Facile "Spotâ€Heating―Synthesis of Carbon Dots/Carbon Nitride for Solar Hydrogen Evolution Synchronously with Contaminant Decomposition. Advanced Functional Materials, 2018, 28, 1706462. | 7.8 | 121 |
| 162 | Enhanced membrane fouling mitigation by modulating cake layer porosity and hydrophilicity in an electro-coagulation/oxidation membrane reactor (ECOMR). Journal of Membrane Science, 2018, 550, 72-79. | 4.1 | 55 |

| # | Article | IF | CITATIONS |
|-----|--|-----|-----------|
| 163 | Ultrafiltration membrane fouling induced by humic acid with typical inorganic salts. Chemosphere, 2018, 197, 793-802. | 4.2 | 40 |
| 164 | Hierarchical Nanotubular Anatase/Rutile/TiO ₂ (B) Heterophase Junction with Oxygen Vacancies for Enhanced Photocatalytic H ₂ Production. Langmuir, 2018, 34, 1883-1889. | 1.6 | 85 |
| 165 | Effects of bromide on the formation and transformation of disinfection by-products during chlorination and chloramination. Science of the Total Environment, 2018, 625, 252-261. | 3.9 | 35 |
| 166 | Tungsten-Assisted Phase Tuning of Molybdenum Carbide for Efficient Electrocatalytic Hydrogen Evolution. ACS Applied Materials & Interfaces, 2018, 10, 2451-2459. | 4.0 | 33 |
| 167 | Interface Stabilization of Undercoordinated Iron Centers on Manganese Oxides for Nature-Inspired Peroxide Activation. ACS Catalysis, 2018, 8, 1090-1096. | 5.5 | 105 |
| 168 | Intensification of anodic charge transfer by contaminant degradation for efficient H ₂ production. Journal of Materials Chemistry A, 2018, 6, 10297-10303. | 5.2 | 28 |
| 169 | Facile Dispersion of Nanosized NiFeP for Highly Effective Catalysis of Oxygen Evolution Reaction. ACS Sustainable Chemistry and Engineering, 2018, 6, 7206-7211. | 3.2 | 46 |
| 170 | Oxidative removal of quinclorac by permanganate through a rate-limiting [3 + 2] cycloaddition reaction. Environmental Sciences: Processes and Impacts, 2018, 20, 790-797. | 1.7 | 11 |
| 171 | Strongly coupled polyoxometalates/oxygen doped g-C3N4 nanocomposites as Fenton-like catalysts for efficient photodegradation of sulfosalicylic acid. Catalysis Communications, 2018, 112, 63-67. | 1.6 | 34 |
| 172 | Fe(II)-regulated moderate pre-oxidation of Microcystis aeruginosa and formation of size-controlled algae flocs for efficient flotation of algae cell and organic matter. Water Research, 2018, 137, 57-63. | 5.3 | 46 |
| 173 | Impacts of water quality on the corrosion of cast iron pipes for water distribution and proposed source water switch strategy. Water Research, 2018, 129, 428-435. | 5.3 | 85 |
| 174 | Comparison of the effects of aluminum and iron(III) salts on ultrafiltration membrane biofouling in drinking water treatment. Journal of Environmental Sciences, 2018, 63, 96-104. | 3.2 | 15 |
| 175 | Determination of pKa and the corresponding structures of quinclorac using combined experimental and theoretical approaches. Journal of Molecular Structure, 2018, 1152, 53-60. | 1.8 | 11 |
| 176 | Specific anion effects on the stability of zeolitic imidazolate framework-8 in aqueous solution. Microporous and Mesoporous Materials, 2018, 259, 171-177. | 2.2 | 50 |
| 177 | Adsorption combined with superconducting high gradient magnetic separation technique used for removal of arsenic and antimony. Journal of Hazardous Materials, 2018, 343, 36-48. | 6.5 | 66 |
| 178 | Oxidation of iopamidol with ferrate (Fe(VI)): Kinetics and formation of toxic iodinated disinfection by-products. Water Research, 2018, 130, 200-207. | 5.3 | 40 |
| 179 | Comparing adsorption of arsenic and antimony from single-solute and bi-solute aqueous systems onto ZIF-8. Colloids and Surfaces A: Physicochemical and Engineering Aspects, 2018, 538, 164-172. | 2.3 | 50 |
| 180 | Rapidly catalysis of oxygen evolution through sequential engineering of vertically layered FeNi structure. Nano Energy, 2018, 43, 359-367. | 8.2 | 49 |

| # | Article | IF | CITATIONS |
|-----|--|------|-----------|
| 181 | Nitrate electro-sorption/reduction in capacitive deionization using a novel Pd/NiAl-layered metal oxide film electrode. Chemical Engineering Journal, 2018, 335, 475-482. | 6.6 | 43 |
| 182 | Deiodination of iopamidol by zero valent iron (ZVI) enhances formation of iodinated disinfection by-products during chloramination. Water Research, 2018, 129, 319-326. | 5.3 | 31 |
| 183 | Fungal Community as a Bioindicator to Reflect Anthropogenic Activities in a River Ecosystem. Frontiers in Microbiology, 2018, 9, 3152. | 1.5 | 34 |
| 184 | Disordering the Atomic Structure of Co(II) Oxide via Bâ€Đoping: An Efficient Oxygen Vacancy Introduction Approach for High Oxygen Evolution Reaction Electrocatalysts. Small, 2018, 14, e1802760. | 5.2 | 88 |
| 185 | Efficient design principle for interfacial charge separation in hydrogen-intercalated nonstoichiometric oxides. Nano Energy, 2018, 53, 887-897. | 8.2 | 27 |
| 186 | Moderate KMnO4-Fe(II) pre-oxidation for alleviating ultrafiltration membrane fouling by algae during drinking water treatment. Water Research, 2018, 142, 96-104. | 5.3 | 51 |
| 187 | Integrated Fe-based floc-membrane process for alleviating ultrafiltration membrane fouling by humic acid and reservoir water. Journal of Membrane Science, 2018, 563, 873-881. | 4.1 | 20 |
| 188 | Site-specific surface tailoring for metal ion selectivity <i>via</i> under-coordinated structure engineering. Nanoscale Horizons, 2018, 3, 632-639. | 4.1 | 3 |
| 189 | Evolving wastewater infrastructure paradigm to enhance harmony with nature. Science Advances, 2018, 4, eaaq0210. | 4.7 | 73 |
| 190 | Oxygen Doping to Optimize Atomic Hydrogen Binding Energy on NiCoP for Highly Efficient Hydrogen Evolution. Small, 2018, 14, e1800421. | 5.2 | 122 |
| 191 | Speciation matching mechanisms between orthophosphate and aluminum species during advanced P removal process. Science of the Total Environment, 2018, 642, 1311-1319. | 3.9 | 13 |
| 192 | Multi-electric field modulation for photocatalytic oxygen evolution: Enhanced charge separation by coupling oxygen vacancies with faceted heterostructures. Nano Energy, 2018, 51, 764-773. | 8.2 | 88 |
| 193 | Reactive, Self-Cleaning Ultrafiltration Membrane Functionalized with Iron Oxychloride Nanocatalysts. Environmental Science & Technology, 2018, 52, 8674-8683. | 4.6 | 124 |
| 194 | Capacitive deionization from reconstruction of NiCoAl-mixed metal oxide film electrode based on the "memory effect― Applied Surface Science, 2018, 459, 767-773. | 3.1 | 16 |
| 195 | Enhanced indirect atomic H* reduction at a hybrid Pd/graphene cathode for electrochemical dechlorination under low negative potentials. Environmental Science: Nano, 2018, 5, 2282-2292. | 2.2 | 57 |
| 196 | Pore Structure-Dependent Mass Transport in Flow-through Electrodes for Water Remediation. Environmental Science & Technology, 2018, 52, 7477-7485. | 4.6 | 36 |
| 197 | Highly efficient and sustainable non-precious-metal Fe–N–C electrocatalysts for the oxygen reduction reaction. Journal of Materials Chemistry A, 2018, 6, 2527-2539. | 5.2 | 214 |
| 198 | Facet-dependent intermediate formation and reaction mechanism of photocatalytic removing hydrophobic anthracene under simulated solar irradiation. Applied Catalysis B: Environmental, 2017, 206, 194-202. | 10.8 | 19 |

| # | Article | IF | CITATIONS |
|-----|---|-----|-----------|
| 199 | Nanostructure-induced colored TiO ₂ array photoelectrodes with full solar spectrum harvesting. Journal of Materials Chemistry A, 2017, 5, 3145-3151. | 5.2 | 19 |
| 200 | Synthesis of Ce(III)-doped Fe3O4 magnetic particles for efficient removal of antimony from aqueous solution. Journal of Hazardous Materials, 2017, 329, 193-204. | 6.5 | 154 |
| 201 | Enhanced degradation of iopamidol by peroxymonosulfate catalyzed by two pipe corrosion products (CuO and δ-MnO 2). Water Research, 2017, 112, 1-8. | 5.3 | 123 |
| 202 | Solvothermal synthesis of BiOI flower-like microspheres for efficient photocatalytic degradation of BPA under visible light irradiation. Catalysis Communications, 2017, 98, 9-12. | 1.6 | 38 |
| 203 | Reductive dechlorination of trichloroacetic acid (TCAA) by electrochemical process over Pd-In/Al2O3 catalyst. Electrochimica Acta, 2017, 232, 13-21. | 2.6 | 52 |
| 204 | Antimony Removal from Aqueous Solution Using Novel α-MnO ₂ Nanofibers: Equilibrium, Kinetic, and Density Functional Theory Studies. ACS Sustainable Chemistry and Engineering, 2017, 5, 2255-2264. | 3.2 | 85 |
| 205 | Identification of Al ₁₃ on the Colloid Surface Using Surface-Enhanced Raman Spectroscopy. Environmental Science & Technology, 2017, 51, 2899-2906. | 4.6 | 13 |
| 206 | Investigating the effect of hardness cations on coagulation: The aspect of neutralisation through Al(III)-dissolved organic matter (DOM) binding. Water Research, 2017, 115, 22-28. | 5.3 | 19 |
| 207 | Preparation of hollow Fe-Al binary metal oxyhydroxide for efficient aqueous fluoride removal. Colloids and Surfaces A: Physicochemical and Engineering Aspects, 2017, 520, 580-589. | 2.3 | 18 |
| 208 | Porous Nanobimetallic Fe–Mn Cubes with High Valent Mn and Highly Efficient Removal of Arsenic(III). ACS Applied Materials & Interfaces, 2017, 9, 14868-14877. | 4.0 | 42 |
| 209 | Degradation of nitro-based pharmaceuticals by UV photolysis: Kinetics and simultaneous reduction on halonitromethanes formation potential. Water Research, 2017, 119, 83-90. | 5.3 | 32 |
| 210 | Enhanced Oxidation of Tetracycline by Permanganate via the Alkali-Induced Alteration of the Highest Occupied Molecular Orbital and the Electrostatic Potential. Industrial & Engineering Chemistry Research, 2017, 56, 4703-4708. | 1.8 | 12 |
| 211 | Synergistic process using Fe hydrolytic flocs and ultrafiltration membrane for enhanced antimony(V) removal. Journal of Membrane Science, 2017, 537, 93-100. | 4.1 | 34 |
| 212 | Simultaneous detection of chlorinated polycyclic aromatic hydrocarbons with polycyclic aromatic hydrocarbons by gas chromatography–mass spectrometry. Analytical and Bioanalytical Chemistry, 2017, 409, 3465-3473. | 1.9 | 12 |
| 213 | Aggregation and Dissociation of Aqueous Al ₁₃ Induced by Fluoride Substitution. Environmental Science & Technology, 2017, 51, 6279-6287. | 4.6 | 16 |
| 214 | Impact of humic acid on the degradation of levofloxacin by aqueous permanganate: Kinetics and mechanism. Water Research, 2017, 123, 67-74. | 5.3 | 101 |
| 215 | Degradation of chloramphenicol by UV/chlorine treatment: Kinetics, mechanism and enhanced formation of halonitromethanes. Water Research, 2017, 121, 178-185. | 5.3 | 144 |
| 216 | Antifouling by pre-deposited Al hydrolytic flocs on ultrafiltration membrane in the presence of humic acid and bovine serum albumin. Journal of Membrane Science, 2017, 538, 34-40. | 4.1 | 19 |

| # | Article | IF | CITATIONS |
|-----|---|-----|-----------|
| 217 | Impact of upgrading wastewater treatment plant on the removal of typical methyl, oxygenated, chlorinated and parent polycyclic aromatic hydrocarbons. Science of the Total Environment, 2017, 603-604, 140-147. | 3.9 | 28 |
| 218 | Enhanced antimony(V) removal using synergistic effects of Fe hydrolytic flocs and ultrafiltration membrane with sludge discharge evaluation. Water Research, 2017, 121, 171-177. | 5.3 | 37 |
| 219 | The removal efficiency and insight into the mechanism of para arsanilic acid adsorption on Fe-Mn framework. Science of the Total Environment, 2017, 601-602, 713-722. | 3.9 | 32 |
| 220 | Boosting photoelectrochemical activities of heterostructured photoanodes through interfacial modulation of oxygen vacancies. Nano Energy, 2017, 35, 290-298. | 8.2 | 59 |
| 221 | Transformation of para arsanilic acid by manganese oxide: Adsorption, oxidation, and influencing factors. Water Research, 2017, 116, 126-134. | 5.3 | 75 |
| 222 | Impact of inner-wall reflection on UV reactor performance as evaluated by using computational fluid dynamics: The role of diffuse reflection. Water Research, 2017, 109, 382-388. | 5.3 | 28 |
| 223 | New Insight into and Characterization of the Aqueous Metal-Enol(ate) Complexes of (Acetonedicarboxylato)copper. ACS Omega, 2017, 2, 6728-6740. | 1.6 | 3 |
| 224 | Enhancing destruction of copper (I) cyanide and subsequent recovery of Cu(I) by a novel electrochemical system combining activated carbon fiber and stainless steel cathodes. Chemical Engineering Journal, 2017, 330, 1187-1194. | 6.6 | 26 |
| 225 | Dual-Functional Ice/Water Interface Allows High-Yield Formation of Al13with Low Energy. ACS Sustainable Chemistry and Engineering, 2017, 5, 8513-8517. | 3.2 | 1 |
| 226 | Influence of microbial community diversity and function on pollutant removal in ecological wastewater treatment. Applied Microbiology and Biotechnology, 2017, 101, 7293-7302. | 1.7 | 12 |
| 227 | Photoactuation Healing of αâ€FeOOH@g ₃ N ₄ Catalyst for Efficient and Stable Activation of Persulfate. Small, 2017, 13, 1702225. | 5.2 | 76 |
| 228 | Melem-based derivatives as metal-free photocatalysts for simultaneous reduction of Cr(VI) and degradation of 5-Sulfosalicylic acid. Journal of Colloid and Interface Science, 2017, 507, 162-171. | 5.0 | 17 |
| 229 | Microbial Interspecies Interactions Affect Arsenic Fate in the Presence of MnII. Microbial Ecology, 2017, 74, 788-794. | 1.4 | 5 |
| 230 | TiO 2 Microflowers Assembled by 6-nm Single-Crystal Stranded Wires with Improved Photoelectrochemical Performances. Electrochimica Acta, 2017, 250, 117-123. | 2.6 | 2 |
| 231 | Oxygen vacancy mediated construction of anatase/brookite heterophase junctions for high-efficiency photocatalytic hydrogen evolution. Journal of Materials Chemistry A, 2017, 5, 24989-24994. | 5.2 | 81 |
| 232 | Light absorption modulation of novel Fe ₂ TiO ₅ inverse opals for photoelectrochemical water splitting. New Journal of Chemistry, 2017, 41, 7966-7971. | 1.4 | 18 |
| 233 | Performance and Mechanisms of Ultrafiltration Membrane Fouling Mitigation by Coupling Coagulation and Applied Electric Field in a Novel Electrocoagulation Membrane Reactor. Environmental Science & Technology, 2017, 51, 8544-8551. | 4.6 | 84 |
| 234 | Unravelling riverine microbial communities under wastewater treatment plant effluent discharge in large urban areas. Applied Microbiology and Biotechnology, 2017, 101, 6755-6764. | 1.7 | 19 |

| # | Article | IF | CITATIONS |
|-----|---|------|-----------|
| 235 | 3D Macroporous Nitrogenâ€Enriched Graphitic Carbon Scaffold for Efficient Bioelectricity Generation in Microbial Fuel Cells. Advanced Energy Materials, 2017, 7, 1601364. | 10.2 | 146 |
| 236 | Adsorption of aromatic organoarsenic compounds by ferric and manganese binary oxide and description of the associated mechanism. Chemical Engineering Journal, 2017, 309, 577-587. | 6.6 | 95 |
| 237 | Combined genotoxicity of chlorinated products from tyrosine and benzophenone-4. Journal of Hazardous Materials, 2017, 322, 387-393. | 6.5 | 7 |
| 238 | Microstructure of carbon nitride affecting synergetic photocatalytic activity: Hydrogen bonds vs. structural defects. Applied Catalysis B: Environmental, 2017, 204, 49-57. | 10.8 | 143 |
| 239 | Microbe–microbe interactions trigger Mn(II)-oxidizing gene expression. ISME Journal, 2017, 11, 67-77. | 4.4 | 39 |
| 240 | Antimony oxidation and adsorption by in-situ formed biogenic Mn oxide and Fe–Mn oxides. Journal of Environmental Sciences, 2017, 54, 126-134. | 3.2 | 49 |
| 241 | Enhanced efficiency in HA removal by electrocoagulation through optimizing flocs properties: Role of current density and pH. Separation and Purification Technology, 2017, 175, 248-254. | 3.9 | 33 |
| 242 | Promoted oxidation of diclofenac with ferrate (Fe(VI)): Role of ABTS as the electron shuttle. Journal of Hazardous Materials, 2017, 336, 65-70. | 6.5 | 32 |
| 243 | Probing Coagulation Behavior of Individual Aluminum Species for Removing Corresponding Disinfection Byproduct Precursors: The Role of Specific Ultraviolet Absorbance. PLoS ONE, 2016, 11, e0148020. | 1.1 | 4 |
| 244 | New Insights into Defectâ€Mediated Heterostructures for Photoelectrochemical Water Splitting. Advanced Energy Materials, 2016, 6, 1502268. | 10.2 | 95 |
| 245 | Magneticallyâ€Confined Feâ€Mn Bimetallic Oxide Encapsulation as an Efficient and Recoverable Adsorbent for Arsenic(III) Removal. Particle and Particle Systems Characterization, 2016, 33, 323-331. | 1.2 | 22 |
| 246 | Enhanced oxidative and adsorptive capability towards antimony by copper-doping into magnetite magnetic particles. RSC Advances, 2016, 6, 66990-67001. | 1.7 | 39 |
| 247 | Utilization of annealed aluminum hydroxide waste with incorporated fluoride for adsorptive removal of heavy metals. Colloids and Surfaces A: Physicochemical and Engineering Aspects, 2016, 504, 95-104. | 2.3 | 6 |
| 248 | Prechlorination of algae-laden water: The effects of transportation time on cell integrity, algal organic matter release, and chlorinated disinfection byproduct formation. Water Research, 2016, 102, 221-228. | 5.3 | 76 |
| 249 | Transformation of humic acid and halogenated byproduct formation in UV-chlorine processes. Water Research, 2016, 102, 421-427. | 5.3 | 164 |
| 250 | Zirconia (ZrO ₂) Embedded in Carbon Nanowires via Electrospinning for Efficient Arsenic Removal from Water Combined with DFT Studies. ACS Applied Materials & Interfaces, 2016, 8, 18912-18921. | 4.0 | 83 |
| 251 | The role of biogenic Fe-Mn oxides formed in situ for arsenic oxidation and adsorption in aquatic ecosystems. Water Research, 2016, 98, 119-127. | 5.3 | 129 |
| 252 | Augmentation of protein-derived acetic acid production by heat-alkaline-induced changes in protein structure and conformation. Water Research, 2016, 88, 595-603. | 5.3 | 41 |

| # | Article | IF | CITATIONS |
|-----|---|------|-----------|
| 253 | Biomolecule-assisted synthesis of defect-mediated Cd _{1â°'x} Zn _x S/MoS ₂ /graphene hollow spheres for highly efficient hydrogen evolution. Physical Chemistry Chemical Physics, 2016, 18, 16208-16215. | 1.3 | 26 |
| 254 | Formation of oxygenated polycyclic aromatic hydrocarbons from polycyclic aromatic hydrocarbons during aerobic activated sludge treatment and their removal process. Chemical Engineering Journal, 2016, 302, 50-57. | 6.6 | 28 |
| 255 | VUV/UV/Chlorine as an Enhanced Advanced Oxidation Process for Organic Pollutant Removal from Water: Assessment with a Novel Mini-Fluidic VUV/UV Photoreaction System (MVPS). Environmental Science & Technology, 2016, 50, 5849-5856. | 4.6 | 76 |
| 256 | Modification of ultrafiltration membrane with iron/aluminum mixed hydrolyzed precipitate layer for humic acid fouling reduction. Desalination and Water Treatment, 2016, 57, 26022-26030. | 1.0 | 1 |
| 257 | Occurrence, distribution, and potential influencing factors of sewage sludge components derived from nine full-scale wastewater treatment plants of Beijing, China. Journal of Environmental Sciences, 2016, 45, 233-239. | 3.2 | 8 |
| 258 | Enhanced formation of bromate and brominated disinfection byproducts during chlorination of bromide-containing waters under catalysis of copper corrosion products. Water Research, 2016, 98, 302-308. | 5.3 | 34 |
| 259 | Efficient conversion of dimethylarsinate into arsenic and its simultaneous adsorption removal over FeCx/N-doped carbon fiber composite in an electro-Fenton process. Water Research, 2016, 100, 57-64. | 5.3 | 71 |
| 260 | Simultaneous surface-adsorbed organic matter desorption and cell integrity maintenance by moderate prechlorination to enhance Microcystis aeruginosa removal in KMnO4Fe(II) process. Water Research, 2016, 105, 551-558. | 5.3 | 38 |
| 261 | Treatment of groundwater containing Mn(II), Fe(II), As(III) and Sb(III) by bioaugmented quartz-sand filters. Water Research, 2016, 106, 126-134. | 5.3 | 73 |
| 262 | Treatment of strongly acidic wastewater with high arsenic concentrations by ferrous sulfide (FeS): Inhibitive effects of S(0)-enriched surfaces. Chemical Engineering Journal, 2016, 304, 986-992. | 6.6 | 74 |
| 263 | Self-assembled one-dimensional MnO ₂ @zeolitic imidazolate framework-8 nanostructures for highly efficient arsenite removal. Environmental Science: Nano, 2016, 3, 1186-1194. | 2.2 | 72 |
| 264 | Natural eggshell membrane as separator for improved coulombic efficiency in air-cathode microbial fuel cells. RSC Advances, 2016, 6, 66147-66151. | 1.7 | 13 |
| 265 | An activated carbon fiber cathode for the degradation of glyphosate in aqueous solutions by the Electro-Fenton mode: Optimal operational conditions and the deposition of iron on cathode on electrode reusability. Water Research, 2016, 105, 575-582. | 5.3 | 99 |
| 266 | Biomass-Derived Porous Fe ₃ C/Tungsten Carbide/Graphitic Carbon Nanocomposite for Efficient Electrocatalysis of Oxygen Reduction. ACS Applied Materials & Interfaces, 2016, 8, 32307-32316. | 4.0 | 88 |
| 267 | Macroporous monolithic Magnéli-phase titanium suboxides as anode material for effective bioelectricity generation in microbial fuel cells. Journal of Materials Chemistry A, 2016, 4, 18002-18007. | 5.2 | 25 |
| 268 | Highly Active and Stable Catalysts of Phytic Acid-Derivative Transition Metal Phosphides for Full Water Splitting. Journal of the American Chemical Society, 2016, 138, 14686-14693. | 6.6 | 647 |
| 269 | Earthâ€Rich Transition Metal Phosphide for Energy Conversion and Storage. Advanced Energy Materials, 2016, 6, 1600087. | 10.2 | 437 |
| 270 | Cooperative Mn(II) oxidation between two bacterial strains in an aquatic environment. Water Research, 2016, 89, 252-260. | 5.3 | 40 |

| # | Article | IF | CITATIONS |
|-----|---|------|-----------|
| 271 | Dechlorination of Trichloroacetic Acid Using a Noble Metal-Free Graphene–Cu Foam Electrode via Direct Cathodic Reduction and Atomic H*. Environmental Science & Technology, 2016, 50, 3829-3837. | 4.6 | 169 |
| 272 | Fabrication of FeOOH hollow microboxes for purification of heavy metal-contaminated water. Physical Chemistry Chemical Physics, 2016, 18, 9437-9445. | 1.3 | 28 |
| 273 | Utilization of aluminum hydroxide waste generated in fluoride adsorption and coagulation processes for adsorptive removal of cadmium ion. Frontiers of Environmental Science and Engineering, 2016, 10, 467-476. | 3.3 | 10 |
| 274 | Two-dimensional layered MoS ₂ : rational design, properties and electrochemical applications. Energy and Environmental Science, 2016, 9, 1190-1209. | 15.6 | 532 |
| 275 | Coagulation behaviors of aluminum salts towards fluoride: Significance of aluminum speciation and transformation. Separation and Purification Technology, 2016, 165, 137-144. | 3.9 | 47 |
| 276 | An effective method for improving electrocoagulation process: Optimization of Al 13 polymer formation. Colloids and Surfaces A: Physicochemical and Engineering Aspects, 2016, 489, 234-240. | 2.3 | 46 |
| 277 | Efficient Nitrate Reduction in a Fluidized Electrochemical Reactor Promoted by Pd–Sn/AC Particles. Catalysis Letters, 2016, 146, 91-99. | 1.4 | 36 |
| 278 | KMnO 4 –Fe(II) pretreatment to enhance Microcystis aeruginosa removal by aluminum coagulation: Does it work after long distance transportation?. Water Research, 2016, 88, 127-134. | 5.3 | 67 |
| 279 | Biomolecule-assisted self-assembly of CdS/MoS 2 /graphene hollow spheres as high-efficiency photocatalysts for hydrogen evolution without noble metals. Applied Catalysis B: Environmental, 2016, 182, 504-512. | 10.8 | 175 |
| 280 | Comparison of Fe–Mn enhanced coagulation and O ₃ -BAC for removing natural organic matter from source waters: a case study. Desalination and Water Treatment, 2016, 57, 9101-9114. | 1.0 | 1 |
| 281 | Contribution of Fe3O4 nanoparticles to the fouling of ultrafiltration with coagulation pre-treatment. Scientific Reports, 2015, 5, 13067. | 1.6 | 11 |
| 282 | Formation of Bi ₂ WO ₆ Bipyramids with Vacancy Pairs for Enhanced Solarâ€Ðriven Photoactivity. Advanced Functional Materials, 2015, 25, 3726-3734. | 7.8 | 155 |
| 283 | Inspection of Feasible Calibration Conditions for <scp>UV</scp> Radiometer Detectors with the <scp>KI</scp> / <scp>KIO</scp> ₃ Actinometer. Photochemistry and Photobiology, 2015, 91, 68-73. | 1.3 | 13 |
| 284 | Enhanced Photoelectrocatalytic Decomposition of Copper Cyanide Complexes and Simultaneous Recovery of Copper with a Bi ₂ MoO ₆ Electrode under Visible Light by EDTA/K ₄ P ₂ O ₇ . Environmental Science & Technology, 2015, 49, 4567-4574. | 4.6 | 45 |
| 285 | Water-based synthesis of zeolitic imidazolate framework-8 with high morphology level at room temperature. RSC Advances, 2015, 5, 48433-48441. | 1.7 | 276 |
| 286 | Defluoridation by Al-based coagulation and adsorption: Species transformation of aluminum and fluoride. Separation and Purification Technology, 2015, 148, 68-75. | 3.9 | 34 |
| 287 | Sulfur-based mixotrophic denitrification corresponding to different electron donors and microbial profiling in anoxic fluidized-bed membrane bioreactors. Water Research, 2015, 85, 422-431. | 5.3 | 134 |
| 288 | Modification of ultrafiltration membrane with nanoscale zerovalent iron layers for humic acid fouling reduction. Water Research, 2015, 71, 140-149. | 5.3 | 53 |

| # | Article | IF | CITATIONS |
|-----|--|-----|-----------|
| 289 | Distribution, mass load and environmental impact of multiple-class pharmaceuticals in conventional and upgraded municipal wastewater treatment plants in East China. Environmental Sciences: Processes and Impacts, 2015, 17, 596-605. | 1.7 | 54 |
| 290 | Denitrification of groundwater using a sulfur-oxidizing autotrophic denitrifying anaerobic fluidized-bed MBR: performance and bacterial community structure. Applied Microbiology and Biotechnology, 2015, 99, 2815-2827. | 1.7 | 109 |
| 291 | Ionic Liquid Assisted Electrospun Cellulose Acetate Fibers for Aqueous Removal of Triclosan. Langmuir, 2015, 31, 1820-1827. | 1.6 | 24 |
| 292 | Elimination of polar micropollutants and anthropogenic markers by wastewater treatment in Beijing, China. Chemosphere, 2015, 119, 1054-1061. | 4.2 | 79 |
| 293 | Probabilistic evaluation of integrating resource recovery into wastewater treatment to improve environmental sustainability. Proceedings of the National Academy of Sciences of the United States of America, 2015, 112, 1630-1635. | 3.3 | 75 |
| 294 | Mechanism of Catalytic Ozonation in Fe ₂ O ₃ /Al ₂ O ₃ @SBA-15 Aqueous Suspension for Destruction of Ibuprofen. Environmental Science & Technology, 2015, 49, 1690-1697. | 4.6 | 286 |
| 295 | Effect of aluminum speciation on ultrafiltration membrane fouling by low dose aluminum coagulation with bovine serum albumin (BSA). Journal of Membrane Science, 2015, 492, 88-94. | 4.1 | 24 |
| 296 | Adsorption of antimony(V) onto Mn(II)-enriched surfaces of manganese-oxide and Fe Mn binary oxide. Chemosphere, 2015, 138, 616-624. | 4.2 | 82 |
| 297 | Cerium incorporated MCM-48 (Ce-MCM-48) as a catalyst to inhibit bromate formation during ozonation of bromide-containing water: Efficacy and mechanism. Water Research, 2015, 86, 2-8. | 5.3 | 37 |
| 298 | Redox Conversion of Chromium(VI) and Arsenic(III) with the Intermediates of Chromium(V) and Arsenic(IV) via AuPd/CNTs Electrocatalysis in Acid Aqueous Solution. Environmental Science & Technology, 2015, 49, 9289-9297. | 4.6 | 91 |
| 299 | Preparation of a manganese dioxide/carbon fiber electrode for electrosorptive removal of copper ions from water. Journal of Colloid and Interface Science, 2015, 446, 359-365. | 5.0 | 63 |
| 300 | UV photolysis kinetics of sulfonamides in aqueous solution based on optimized fluence quantification. Water Research, 2015, 75, 43-50. | 5.3 | 67 |
| 301 | Highly Efficient AuPd/Carbon Nanotube Nanocatalysts for the Electroâ€Fenton Process. Chemistry - A European Journal, 2015, 21, 7611-7620. | 1.7 | 30 |
| 302 | Coagulation of methylated arsenic from drinking water: Influence of methyl substitution. Journal of Hazardous Materials, 2015, 293, 97-104. | 6.5 | 30 |
| 303 | Removal of tetracycline antibiotics from aqueous solution by amino-Fe (III) functionalized SBA15. Colloids and Surfaces A: Physicochemical and Engineering Aspects, 2015, 471, 133-138. | 2.3 | 113 |
| 304 | Photocatalytic mineralisation of herbicide 2,4,5-trichlorophenoxyacetic acid: enhanced performance by triple junction Cu–TiO ₂ –Cu ₂ O and the underlying reaction mechanism. New Journal of Chemistry, 2015, 39, 314-320. | 1.4 | 44 |
| 305 | Iron-incorporated mesoporous silica for enhanced adsorption of tetracycline in aqueous solution. RSC Advances, 2015, 5, 42407-42413. | 1.7 | 32 |
| 306 | Graphene-modified Pd/C cathode and Pd/GAC particles for enhanced electrocatalytic removal of bromate in a continuous three-dimensional electrochemical reactor. Water Research, 2015, 77, 1-12. | 5.3 | 100 |

Jiuнui Qu

| # | Article | IF | CITATIONS |
|-----|--|-----|-----------|
| 307 | Microfluidic Flow through Polyaniline Supported by Lamellar-Structured Graphene for Mass-Transfer-Enhanced Electrocatalytic Reduction of Hexavalent Chromium. Environmental Science & Technology, 2015, 49, 13534-13541. | 4.6 | 98 |
| 308 | Electric Double-Layer Effects Induce Separation of Aqueous Metal Ions. ACS Nano, 2015, 9, 10922-10930. | 7.3 | 43 |
| 309 | Reusability of Al-F Hydroxide Precipitates Generated in Adsorption and Coagulation Treatment of Fluoride for Adsorptive Removal of Arsenic. Environmental Engineering Science, 2015, 32, 613-621. | 0.8 | 3 |
| 310 | Photoelectrocatalytic Oxidation of Cu-cyanides and Cu-EDTA at TiO2 nanotube electrode. Electrochimica Acta, 2015, 180, 129-137. | 2.6 | 44 |
| 311 | Removal of Antimonite (Sb(III)) and Antimonate (Sb(V)) from Aqueous Solution Using Carbon Nanofibers That Are Decorated with Zirconium Oxide (ZrO ₂). Environmental Science & Technology, 2015, 49, 11115-11124. | 4.6 | 233 |
| 312 | Simultaneous removal of Cd(II) and Sb(V) by Fe–Mn binary oxide: Positive effects of Cd(II) on Sb(V) adsorption. Journal of Hazardous Materials, 2015, 300, 847-854. | 6.5 | 88 |
| 313 | A Mini-Fluidic UV Photoreaction System for Bench-Scale Photochemical Studies. Environmental Science and Technology Letters, 2015, 2, 297-301. | 3.9 | 8 |
| 314 | AuPd/Fe3O4-based three-dimensional electrochemical system for efficiently catalytic degradation of 1-butyl-3-methylimidazolium hexafluorophosphate. Electrochimica Acta, 2015, 186, 328-336. | 2.6 | 37 |
| 315 | Chlorination of tramadol: Reaction kinetics, mechanism and genotoxicity evaluation. Chemosphere, 2015, 141, 282-289. | 4.2 | 26 |
| 316 | Adsorption of Sb(III) and Sb(V) on Freshly Prepared Ferric Hydroxide (FeOxHy). Environmental Engineering Science, 2015, 32, 95-102. | 0.8 | 61 |
| 317 | Permanganate oxidation of diclofenac: The pH-dependent reaction kinetics and a ring-opening mechanism. Chemosphere, 2015, 136, 297-304. | 4.2 | 47 |
| 318 | Visible-Light Induced Photocatalytic Activity of Electrospun-TiO ₂ in Arsenic(III) Oxidation. ACS Applied Materials & Interfaces, 2015, 7, 511-518. | 4.0 | 42 |
| 319 | Heterogeneous photo-Fenton degradation of acid red B over Fe2O3 supported on activated carbon fiber. Journal of Hazardous Materials, 2015, 285, 167-172. | 6.5 | 147 |
| 320 | Simultaneous removal of arsenic and fluoride by freshly-prepared aluminum hydroxide. Colloids and Surfaces A: Physicochemical and Engineering Aspects, 2015, 466, 147-153. | 2.3 | 28 |
| 321 | Comparing the adsorption behaviors of Cd, Cu and Pb from water onto Fe-Mn binary oxide, MnO2 and FeOOH. Frontiers of Environmental Science and Engineering, 2015, 9, 385-393. | 3.3 | 43 |
| 322 | Reaction of aqueous Cu–Citrate with MnO2 birnessite: Characterization of Mn dissolution, oxidation products and surface interactions. Chemosphere, 2015, 119, 1-7. | 4.2 | 25 |
| 323 | Graphene-based transition metal oxide nanocomposites for the oxygen reduction reaction. Nanoscale, 2015, 7, 1250-1269. | 2.8 | 290 |
| 324 | Metagenomic Approach Reveals Variation of Microbes with Arsenic and Antimony Metabolism Genes from Highly Contaminated Soil. PLoS ONE, 2014, 9, e108185. | 1.1 | 75 |

| # | Article | IF | CITATIONS |
|-----|--|------|-----------|
| 325 | Comparison of iron (III) and alum salt on ultrafiltration membrane fouling by alginate. Desalination, 2014, 354, 153-159. | 4.0 | 19 |
| 326 | Enhanced destruction of Cu(CN)32â^' by H2O2 under alkaline conditions in the presence of EDTA/pyrophosphate. Chemical Engineering Journal, 2014, 253, 478-485. | 6.6 | 26 |
| 327 | Investigation of pre-coagulation and powder activate carbon adsorption on ultrafiltration membrane fouling. Journal of Membrane Science, 2014, 459, 157-168. | 4.1 | 67 |
| 328 | Organic micropollutants in the Yangtze River: Seasonal occurrence and annual loads. Science of the Total Environment, 2014, 472, 789-799. | 3.9 | 102 |
| 329 | Electrochemical removal of haloacetic acids in a three-dimensional electrochemical reactor with Pd-GAC particles as fixed filler and Pd-modified carbon paper as cathode. Water Research, 2014, 51, 134-143. | 5.3 | 68 |
| 330 | Investigation of the property of kaolin–alum flocs at acidic pH. Colloids and Surfaces A: Physicochemical and Engineering Aspects, 2014, 443, 177-181. | 2.3 | 12 |
| 331 | Using high-throughput sequencing to assess the impacts of treated and untreated wastewater discharge on prokaryotic communities in an urban river. Applied Microbiology and Biotechnology, 2014, 98, 1841-1851. | 1.7 | 63 |
| 332 | Occurrence, behavior and removal of typical substituted and parent polycyclic aromatic hydrocarbons in a biological wastewater treatmentÂplant. Water Research, 2014, 52, 11-19. | 5.3 | 68 |
| 333 | Oxygenated, nitrated, methyl and parent polycyclic aromatic hydrocarbons in rivers of Haihe River System, China: Occurrence, possible formation, and source and fate in a water-shortage area. Science of the Total Environment, 2014, 481, 178-185. | 3.9 | 85 |
| 334 | Determination of rapid chlorination rate constants by a stopped-flow spectrophotometric competition kinetics method. Water Research, 2014, 55, 126-132. | 5.3 | 20 |
| 335 | Electrochemical Reduction of Bromate by a Pd Modified Carbon Fiber Electrode: Kinetics and Mechanism. Electrochimica Acta, 2014, 132, 151-157. | 2.6 | 23 |
| 336 | Efficient electrochemical reduction of bromate by a Pd/rGO/CFP electrode with low applied potentials. Applied Catalysis B: Environmental, 2014, 160-161, 179-187. | 10.8 | 60 |
| 337 | Simultaneous destruction of Nickel (II)-EDTA with TiO2/Ti film anode and electrodeposition of nickel ions on the cathode. Applied Catalysis B: Environmental, 2014, 144, 478-485. | 10.8 | 95 |
| 338 | Effect of low dosage of coagulant on the ultrafiltration membrane performance in feedwater treatment. Water Research, 2014, 51, 277-283. | 5.3 | 60 |
| 339 | Fragmentation of typical sulfonamide drugs via heterolytic bond cleavage and stepwise rearrangement. RSC Advances, 2014, 4, 48426-48432. | 1.7 | 25 |
| 340 | Metagenomic analysis reveals microbial diversity and function in the rhizosphere soil of a constructed wetland. Environmental Technology (United Kingdom), 2014, 35, 2521-2527. | 1.2 | 52 |
| 341 | Mn(VII)–Fe(II) pre-treatment for Microcystis aeruginosa removal by Al coagulation: Simultaneous enhanced cyanobacterium removal and residual coagulant control. Water Research, 2014, 65, 73-84. | 5.3 | 48 |
| 342 | Respective Role of Fe and Mn Oxide Contents for Arsenic Sorption in Iron and Manganese Binary Oxide: An X-ray Absorption Spectroscopy Investigation. Environmental Science & Technology, 2014, 48, 10316-10322. | 4.6 | 200 |

| # | Article | IF | CITATIONS |
|-----|--|------|-----------|
| 343 | Adsorption behavior of sulfamethazine in an activated sludge process treating swine wastewater. Journal of Environmental Sciences, 2014, 26, 1623-1629. | 3.2 | 39 |
| 344 | Facile Synthesis of Graphite-Reduced Graphite Oxide Core–Sheath Fiber via Direct Exfoliation of Carbon Fiber for Supercapacitor Application. ACS Applied Materials & Interfaces, 2014, 6, 9496-9502. | 4.0 | 30 |
| 345 | Characterization of dissolved organic matter from surface waters with low to high dissolved organic carbon and the related disinfection byproduct formation potential. Journal of Hazardous Materials, 2014, 271, 228-235. | 6.5 | 54 |
| 346 | α-Fe ₂ O ₃ spherical nanocrystals supported on CNTs as efficient non-noble electrocatalysts for the oxygen reduction reaction. Journal of Materials Chemistry A, 2014, 2, 13635-13640. | 5.2 | 110 |
| 347 | Inhibition of bromate formation by surface reduction in catalytic ozonation of organic pollutants over β-FeOOH/Al2O3. Applied Catalysis B: Environmental, 2014, 147, 287-292. | 10.8 | 64 |
| 348 | Characterization of biofilm and corrosion of cast iron pipes in drinking water distribution system with UV/Cl2 disinfection. Water Research, 2014, 60, 174-181. | 5.3 | 101 |
| 349 | Reaction of Cu(CN)32â^' with H2O2 in water under alkaline conditions: Cyanide oxidation, Cu+/Cu2+ catalysis and H2O2 decomposition. Applied Catalysis B: Environmental, 2014, 158-159, 85-90. | 10.8 | 66 |
| 350 | Characterization and reactivity of biogenic manganese oxides for ciprofloxacin oxidation. Journal of Environmental Sciences, 2014, 26, 1154-1161. | 3.2 | 60 |
| 351 | Phosphate removal from water using freshly formed Fe–Mn binary oxide: Adsorption behaviors and mechanisms. Colloids and Surfaces A: Physicochemical and Engineering Aspects, 2014, 455, 11-18. | 2.3 | 117 |
| 352 | Photoelectrocatalytic oxidation of Cu-EDTA complex and electrodeposition recovery of Cu in a continuous tubular photoelectrochemical reactor. Chemical Engineering Journal, 2014, 239, 53-59. | 6.6 | 65 |
| 353 | Synthesis of carbon-coated magnetic nanocomposite (Fe3O4@C) and its application for sulfonamide antibiotics removal from water. Journal of Environmental Sciences, 2014, 26, 962-969. | 3.2 | 94 |
| 354 | Characterization and adsorption performance of Zrâ€doped akaganéite for efficient arsenic removal. Journal of Chemical Technology and Biotechnology, 2013, 88, 629-635. | 1.6 | 40 |
| 355 | The pre-treatment of submerged ultrafiltration membrane by coagulation—Effect of polyacrylamide as a coagulant aid. Journal of Membrane Science, 2013, 446, 50-58. | 4.1 | 53 |
| 356 | Polycyclic aromatic hydrocarbons in wastewater, WWTPs effluents and in the recipient waters of Beijing, China. Environmental Science and Pollution Research, 2013, 20, 4254-4260. | 2.7 | 50 |
| 357 | Species distribution of arsenic in sediments after an unexpected emergent discharge of high-arsenic wastewater into a river. Frontiers of Environmental Science and Engineering, 2013, 7, 568-578. | 3.3 | 5 |
| 358 | Preparation and evaluation of Zr-β-FeOOH for efficient arsenic removal. Journal of Environmental Sciences, 2013, 25, 815-822. | 3.2 | 18 |
| 359 | Comparison of submerged coagulation and traditional coagulation on membrane fouling: Effect of active flocs. Desalination, 2013, 309, 11-17. | 4.0 | 16 |
| 360 | Disinfection by-products formation and precursors transformation during chlorination and chloramination of highly-polluted source water: Significance of ammonia. Water Research, 2013, 47, 5901-5910. | 5.3 | 72 |

| # | Article | IF | CITATIONS |
|-----|--|------|-----------|
| 361 | Removal of arsenic(III) from aqueous solution using a low-cost by-product in Fe-removal plants—Fe-based backwashing sludge. Chemical Engineering Journal, 2013, 226, 393-401. | 6.6 | 57 |
| 362 | Simultaneous determination of typical substituted and parent polycyclic aromatic hydrocarbons in water and solid matrix by gas chromatography–mass spectrometry. Journal of Chromatography A, 2013, 1291, 129-136. | 1.8 | 37 |
| 363 | Effect of iron/aluminum hydrolyzed precipitate layer on ultrafiltration membrane. Desalination, 2013, 330, 16-21. | 4.0 | 23 |
| 364 | Effects of fluoride on coagulation performance of aluminum chloride towards Kaolin suspension. Colloids and Surfaces A: Physicochemical and Engineering Aspects, 2013, 421, 84-90. | 2.3 | 28 |
| 365 | Photoelectrocatalytic Oxidation of Cu ^{II} –EDTA at the TiO ₂ Electrode and Simultaneous Recovery of Cu ^{II} by Electrodeposition. Environmental Science & Technology, 2013, 47, 4480-4488. | 4.6 | 151 |
| 366 | Adsorptive removal of phosphate by a nanostructured Fe–Al–Mn trimetal oxide adsorbent. Powder Technology, 2013, 233, 146-154. | 2.1 | 268 |
| 367 | Chlorination and chloramination of high-bromide natural water: DBPs species transformation. Separation and Purification Technology, 2013, 102, 86-93. | 3.9 | 49 |
| 368 | Efficient treatment of an electroplating wastewater containing heavy metal ions, cyanide, and organics by H2O2 oxidation followed by the anodic Fenton process. Water Science and Technology, 2013, 68, 1329-1335. | 1.2 | 19 |
| 369 | Integrated Metagenomic and Physiochemical Analyses to Evaluate the Potential Role of Microbes in the Sand Filter of a Drinking Water Treatment System. PLoS ONE, 2013, 8, e61011. | 1.1 | 64 |
| 370 | Research Progress of Biogenic Manganese Oxides and Application Potential in Water Treatment Process. Ying Yong Yu Huan Jing Sheng Wu Xue Bao = Chinese Journal of Applied and Environmental Biology, 2013, 19, 11-19. | 0.1 | 1 |
| 371 | Arsenic Desorption from Ferric and Manganese Binary Oxide by Competitive Anions: Significance of pH. Water Environment Research, 2012, 84, 521-528. | 1.3 | 12 |
| 372 | Efficient Removal of Toxic Pollutants Over Fe–Co/ZrO2 Bimetallic Catalyst with Ozone. Catalysis Letters, 2012, 142, 1026-1032. | 1.4 | 11 |
| 373 | As(III) Oxidation by Active Chlorine and Subsequent Removal of As(V) by Al ₁₃ Polymer Coagulation Using a Novel Dual Function Reagent. Environmental Science & Technology, 2012, 46, 6776-6782. | 4.6 | 42 |
| 374 | Effect of moderate pre-oxidation on the removal of Microcystis aeruginosa by KMnO4–Fe(II) process: Significance of the in-situ formed Fe(III). Water Research, 2012, 46, 73-81. | 5.3 | 107 |
| 375 | Effects of disinfectant and biofilm on the corrosion of cast iron pipes in a reclaimed water distribution system. Water Research, 2012, 46, 1070-1078. | 5.3 | 193 |
| 376 | Enhanced Fenton degradation of Rhodamine B over nanoscaled Cu-doped LaTiO3 perovskite. Applied Catalysis B: Environmental, 2012, 125, 418-424. | 10.8 | 174 |
| 377 | Combination of electroreduction with biosorption for enhancement for removal of hexavalent chromium. Journal of Colloid and Interface Science, 2012, 385, 147-153. | 5.0 | 29 |
| 378 | Adsorption of nitrate and nitrite from aqueous solution onto calcined (Mg–Al) hydrotalcite of different Mg/Al ratio. Chemical Engineering Journal, 2012, 195-196, 241-247. | 6.6 | 123 |

| # | Article | IF | CITATIONS |
|-----|---|------|-----------|
| 379 | Optimization of chlorine-based disinfection for the control of disinfection by-products formation and CODMn: A case study. Chemical Engineering Journal, 2012, 197, 116-122. | 6.6 | 9 |
| 380 | Characterization of flocs generated by preformed and in situ formed Al13 polymer. Chemical Engineering Journal, 2012, 197, 10-15. | 6.6 | 30 |
| 381 | Enhanced Photodegradation of Toxic Pollutants on Plasmonic Au–Ag–AgI/Al2O3 Under Visible Irradiation. Catalysis Letters, 2012, 142, 646-654. | 1.4 | 14 |
| 382 | Catalyzing denitrification of Paracoccus versutus by immobilized 1,5-dichloroanthraquinone. Biodegradation, 2012, 23, 399-405. | 1.5 | 15 |
| 383 | The electrocatalytic dechlorination of chloroacetic acids at electrodeposited Pd/Fe-modified carbon paper electrode. Applied Catalysis B: Environmental, 2012, 111-112, 628-635. | 10.8 | 120 |
| 384 | Effect of aluminum fluoride complexation on fluoride removal by coagulation. Colloids and Surfaces A: Physicochemical and Engineering Aspects, 2012, 395, 88-93. | 2.3 | 112 |
| 385 | Effect of dosage strategy on Al-humic flocs growth and re-growth. Colloids and Surfaces A: Physicochemical and Engineering Aspects, 2012, 404, 106-111. | 2.3 | 31 |
| 386 | Arsenate uptake and arsenite simultaneous sorption and oxidation by Fe–Mn binary oxides: Influence of Mn/Fe ratio, pH, Ca2+, and humic acid. Journal of Colloid and Interface Science, 2012, 366, 141-146. | 5.0 | 108 |
| 387 | Bromate removal by electrochemical reduction at boron-doped diamond electrode. Electrochimica Acta, 2012, 62, 181-184. | 2.6 | 53 |
| 388 | Biological catalyzed denitrification by a functional electropolymerization biocarrier modified by redox mediator. Bioresource Technology, 2012, 107, 144-150. | 4.8 | 33 |
| 389 | Removal of tetracycline from water by Fe-Mn binary oxide. Journal of Environmental Sciences, 2012, 24, 242-247. | 3.2 | 125 |
| 390 | Optimum conditions for the formation of Al13 polymer and active chlorine in electrolysis process with Ti/RuO2-TiO2 anodes. Journal of Environmental Sciences, 2012, 24, 297-302. | 3.2 | 7 |
| 391 | Removal of natural organic matter for controlling disinfection by-products formation by enhanced coagulation: A case study. Separation and Purification Technology, 2012, 84, 41-45. | 3.9 | 41 |
| 392 | Effects and mechanisms of pre-chlorination on Microcystis aeruginosa removal by alum coagulation: Significance of the released intracellular organic matter. Separation and Purification Technology, 2012, 86, 19-25. | 3.9 | 135 |
| 393 | Effect of aluminum speciation on arsenic removal during coagulation process. Separation and Purification Technology, 2012, 86, 35-40. | 3.9 | 86 |
| 394 | Simultaneous removal of arsenate and fluoride by iron and aluminum binary oxide: Competitive adsorption effects. Separation and Purification Technology, 2012, 92, 100-105. | 3.9 | 59 |
| 395 | Chlorination of Microcystis aeruginosa suspension: Cell lysis, toxin release and degradation. Journal of Hazardous Materials, 2012, 217-218, 279-285. | 6.5 | 95 |
| 396 | Partitioning and sources of PAHs in wastewater receiving streams of Tianjin, China. Environmental Monitoring and Assessment, 2012, 184, 1847-1855. | 1.3 | 9 |

| # | Article | IF | CITATIONS |
|-----|--|-----|-----------|
| 397 | Improvement of metal adsorption onto chitosan/Sargassum sp. composite sorbent by an innovative ion-imprint technology. Water Research, 2011, 45, 145-154. | 5.3 | 152 |
| 398 | Characteristic transformation of humic acid during photoelectrocatalysis process and its subsequent disinfection byproduct formation potential. Water Research, 2011, 45, 6131-6140. | 5.3 | 78 |
| 399 | Fabrication and photoelectrocatalytic properties of nanocrystalline monoclinic BiVO4 thin-film electrode. Journal of Environmental Sciences, 2011, 23, 151-159. | 3.2 | 52 |
| 400 | Removal of bentazone from micro-polluted water using MIEX resin: Kinetics, equilibrium, and mechanism. Journal of Environmental Sciences, 2011, 23, 381-387. | 3.2 | 33 |
| 401 | Photoelectrochemical degradation of Methylene Blue with β-PbO2 electrodes driven by visible light irradiation. Journal of Environmental Sciences, 2011, 23, 998-1003. | 3.2 | 39 |
| 402 | Development of systems for detection, early warning, and control of pipeline leakage in drinking water distribution: A case study. Journal of Environmental Sciences, 2011, 23, 1816-1822. | 3.2 | 55 |
| 403 | The mechanism of antimony(III) removal and its reactions on the surfaces of Fe–Mn Binary Oxide. Journal of Colloid and Interface Science, 2011, 363, 320-326. | 5.0 | 230 |
| 404 | Study of a combined sulfur autotrophic with proton-exchange membrane electrodialytic denitrification technology: Sulfate control and pH balance. Bioresource Technology, 2011, 102, 10803-10809. | 4.8 | 17 |
| 405 | Defluoridation by freshly prepared aluminum hydroxides. Chemical Engineering Journal, 2011, 175, 144-149. | 6.6 | 57 |
| 406 | Arsenic release from arsenic-bearing Fe–Mn binary oxide: Effects of Eh condition. Chemosphere, 2011, 83, 1020-1027. | 4.2 | 32 |
| 407 | Polycyclic aromatic hydrocarbons in effluents from wastewater treatment plants and receiving streams in Tianjin, China. Environmental Monitoring and Assessment, 2011, 177, 467-480. | 1.3 | 22 |
| 408 | PAH desorption from sediments with different contents of organic carbon from wastewater receiving rivers. Environmental Science and Pollution Research, 2011, 18, 346-354. | 2.7 | 17 |
| 409 | Migration of manganese and iron during the adsorption-regeneration cycles for arsenic removal. Frontiers of Environmental Science and Engineering in China, 2011, 5, 512-518. | 0.8 | 1 |
| 410 | Aluminum speciation of coagulants with low concentration: Analysis by electrospray ionization mass spectrometry. Colloids and Surfaces A: Physicochemical and Engineering Aspects, 2011, 379, 43-50. | 2.3 | 27 |
| 411 | Photoelectrocatalytic degradation of organic contaminants at Bi2O3/TiO2 nanotube array electrode. Applied Surface Science, 2011, 257, 4621-4624. | 3.1 | 69 |
| 412 | Arsenic removal from a high-arsenic wastewater using in situ formed Fe–Mn binary oxide combined with coagulation by poly-aluminum chloride. Journal of Hazardous Materials, 2011, 185, 990-995. | 6.5 | 33 |
| 413 | Photodegradation and toxicity changes of antibiotics in UV and UV/H2O2 process. Journal of Hazardous Materials, 2011, 185, 1256-1263. | 6.5 | 240 |
| 414 | Formation of disinfection by-products in the chlorination of ammonia-containing effluents: Significance of Cl2/N ratios and the DOM fractions. Journal of Hazardous Materials, 2011, 190, 645-651. | 6.5 | 27 |

| # | Article | IF | CITATIONS |
|-----|--|------|-----------|
| 415 | Application of nuclear magnetic resonance spectroscopy, Fourier transform infrared spectroscopy, UV–Visible spectroscopy and kinetic modeling for elucidation of adsorption chemistry in uptake of tetracycline by zeolite beta. Journal of Colloid and Interface Science, 2011, 354, 261-267. | 5.0 | 65 |
| 416 | Arsenic(III,V) Adsorption on Iron-Oxide-Coated Manganese Sand and Quartz Sand: Comparison of Different Carriers and Adsorption Capacities. Environmental Engineering Science, 2011, 28, 643-651. | 0.8 | 30 |
| 417 | Arsenic Species Transformation and Transportation in Arsenic Removal by Fe-Mn Binary Oxide–Coated Diatomite: Pilot-Scale Field Study. Journal of Environmental Engineering, ASCE, 2011, 137, 1122-1127. | 0.7 | 14 |
| 418 | Effect of chlorination and ozone pre-oxidation on the photobacteria acute toxicity for dissolved organic matter from sewage treatment plants. Scientia Sinica Chimica, 2011, 41, 91-96. | 0.2 | 0 |
| 419 | Degradation characteristics of humic acid over iron oxides/FeO core–shell nanoparticles with UVA/H2O2. Journal of Hazardous Materials, 2010, 173, 474-479. | 6.5 | 50 |
| 420 | Treatment of dye wastewater with permanganate oxidation and in situ formed manganese dioxides adsorption: Cation blue as model pollutant. Journal of Hazardous Materials, 2010, 176, 926-931. | 6.5 | 42 |
| 421 | Effect of chlorination and ozone pre-oxidation on the photobacteria acute toxicity for dissolved organic matter from sewage treatment plants. Science China Chemistry, 2010, 53, 2394-2398. | 4.2 | 5 |
| 422 | Practical performance and its efficiency of arsenic removal from groundwater using Fe-Mn binary oxide. Journal of Environmental Sciences, 2010, 22, 1-6. | 3.2 | 43 |
| 423 | Bioâ€electrochemical denitrification by a novel protonâ€exchange membrane electrodialysis system—a batch mode study. Journal of Chemical Technology and Biotechnology, 2010, 85, 1540-1546. | 1.6 | 7 |
| 424 | Catalytic ozonation of toxic pollutants over magnetic cobalt and manganese co-doped γ-Fe2O3. Applied Catalysis B: Environmental, 2010, 100, 62-67. | 10.8 | 131 |
| 425 | Systematic study of synergistic and antagonistic effects on adsorption of tetracycline and copper onto a chitosan. Journal of Colloid and Interface Science, 2010, 344, 117-125. | 5.0 | 229 |
| 426 | Removal of arsenite by simultaneous electro-oxidation and electro-coagulation process. Journal of Hazardous Materials, 2010, 184, 472-476. | 6.5 | 78 |
| 427 | Surface acidity and reactivity of β-FeOOH/Al2O3 for pharmaceuticals degradation with ozone: In situ ATR-FTIR studies. Applied Catalysis B: Environmental, 2010, 97, 340-346. | 10.8 | 118 |
| 428 | Visible-light sensitive cobalt-doped BiVO4 (Co-BiVO4) photocatalytic composites for the degradation of methylene blue dye in dilute aqueous solutions. Applied Catalysis B: Environmental, 2010, 99, 214-221. | 10.8 | 285 |
| 429 | The Current State of Water Quality and Technology Development for Water Pollution Control in China. Critical Reviews in Environmental Science and Technology, 2010, 40, 519-560. | 6.6 | 207 |
| 430 | Plasmon-Induced Photodegradation of Toxic Pollutants with Agâ^'AgI/Al ₂ O ₃ under Visible-Light Irradiation. Journal of the American Chemical Society, 2010, 132, 857-862. | 6.6 | 541 |
| 431 | Plasmon-Induced Inactivation of Enteric Pathogenic Microorganisms with Agâ°`Agl/Al ₂ O ₃ under Visible-Light Irradiation. Environmental Science & Technology, 2010, 44, 7058-7062. | 4.6 | 76 |
| 432 | Plasmon-Assisted Degradation of Toxic Pollutants with Agâ^'AgBr/Al ₂ O ₃ under Visible-Light Irradiation. Journal of Physical Chemistry C, 2010, 114, 2746-2750. | 1.5 | 186 |

| # | Article | IF | CITATIONS |
|-----|--|-----|-----------|
| 433 | Photoelectrocatalytic degradation of organic contaminant at hybrid BDD-ZnWO4 electrode. Catalysis Communications, 2010, 12, 76-79. | 1.6 | 15 |
| 434 | The influence of colloids on the geochemical behavior of metals in polluted water using as an example Yongdingxin River, Tianjin, China. Chemosphere, 2010, 78, 360-367. | 4.2 | 33 |
| 435 | Adsorption and removal of arsenite on ordered mesoporous Fe-modified ZrO ₂ . Desalination and Water Treatment, 2009, 8, 139-145. | 1.0 | 19 |
| 436 | The effects of different nitrogen compounds on the growth and microcystin production of Microcystis aeruginosa. Journal of Water Supply: Research and Technology - AQUA, 2009, 58, 277-284. | 0.6 | 4 |
| 437 | Electro-photocatalytic degradation of acid orange II using a novel TiO2/ACF photoanode. Science of the Total Environment, 2009, 407, 2431-2439. | 3.9 | 55 |
| 438 | Mechanism of Cu(II)-catalyzed monochloramine decomposition in aqueous solution. Science of the Total Environment, 2009, 407, 4105-4109. | 3.9 | 14 |
| 439 | The progress of catalytic technologies in water purification: A review. Journal of Environmental Sciences, 2009, 21, 713-719. | 3.2 | 102 |
| 440 | Electrochemical incineration of dimethyl phthalate by anodic oxidation with boron-doped diamond electrode. Journal of Environmental Sciences, 2009, 21, 1321-1328. | 3.2 | 31 |
| 441 | Preparation of organically functionalized silica gel as adsorbent for copper ion adsorption. Journal of Environmental Sciences, 2009, 21, 1473-1479. | 3.2 | 56 |
| 442 | Characterization of dissolved organic matter fractions and its relationship with the disinfection by-product formation. Journal of Environmental Sciences, 2009, 21, 54-61. | 3.2 | 28 |
| 443 | Pilotâ€scale treatment of wasteâ€water from carbon production by a combined physical–chemical process. Journal of Chemical Technology and Biotechnology, 2009, 84, 966-971. | 1.6 | 5 |
| 444 | Fabrication of TiO2/Ti nanotube electrode and the photoelectrochemical behaviors in NaCl solutions. Journal of Solid State Electrochemistry, 2009, 13, 1959-1964. | 1.2 | 11 |
| 445 | Electro-oxidation of diclofenac at boron doped diamond: Kinetics and mechanism. Electrochimica Acta, 2009, 54, 4172-4179. | 2.6 | 93 |
| 446 | Control of health risks in drinking water through point-of-use systems. Science Bulletin, 2009, 54, 1996-2001. | 4.3 | 2 |
| 447 | Effects of amino acids on microcystin production of the Microcystis aeruginosa. Journal of Hazardous Materials, 2009, 161, 730-736. | 6.5 | 70 |
| 448 | Characterization of isolated fractions of dissolved organic matter from sewage treatment plant and the related disinfection by-products formation potential. Journal of Hazardous Materials, 2009, 164, 1433-1438. | 6.5 | 137 |
| 449 | Adsorption behavior and mechanism of arsenate at Fe–Mn binary oxide/water interface. Journal of Hazardous Materials, 2009, 168, 820-825. | 6.5 | 194 |
| 450 | Study of a combined heterotrophic and sulfur autotrophic denitrification technology for removal of nitrate in water. Journal of Hazardous Materials, 2009, 169, 23-28. | 6.5 | 121 |

| # | Article | IF | CITATIONS |
|-----|---|------|-----------|
| 451 | Cu(II)-catalyzed THM formation during water chlorination and monochloramination: A comparison study. Journal of Hazardous Materials, 2009, 170, 58-65. | 6.5 | 34 |
| 452 | Effect of pH on the aluminum salts hydrolysis during coagulation process: Formation and decomposition of polymeric aluminum species. Journal of Colloid and Interface Science, 2009, 330, 105-112. | 5.0 | 113 |
| 453 | Effects of calcium ions on surface characteristics and adsorptive properties of hydrous manganese dioxide. Journal of Colloid and Interface Science, 2009, 331, 275-280. | 5.0 | 72 |
| 454 | Role of the Mg/Al atomic ratio in hydrotalcite-supported Pd/Sn catalysts for nitrate adsorption and hydrogenation reduction. Journal of Colloid and Interface Science, 2009, 332, 151-157. | 5.0 | 44 |
| 455 | k-Value-based ferron assay and its application. Journal of Colloid and Interface Science, 2009, 335, 44-49. | 5.0 | 14 |
| 456 | Removal of phosphate from water by a Fe–Mn binary oxide adsorbent. Journal of Colloid and Interface Science, 2009, 335, 168-174. | 5.0 | 356 |
| 457 | Fe–Mn binary oxide incorporated into diatomite as an adsorbent for arsenite removal: Preparation and evaluation. Journal of Colloid and Interface Science, 2009, 338, 353-358. | 5.0 | 99 |
| 458 | Coagulation of humic acid by PACI with high content of Al13: The role of aluminum speciation. Separation and Purification Technology, 2009, 70, 225-230. | 3.9 | 93 |
| 459 | Photoelectrochemical degradation of anti-inflammatory pharmaceuticals at Bi2MoO6–boron-doped diamond hybrid electrode under visible light irradiation. Applied Catalysis B: Environmental, 2009, 91, 539-545. | 10.8 | 84 |
| 460 | Photoassisted degradation of endocrine disruptors over CuOx–FeOOH with H2O2 at neutral pH. Applied Catalysis B: Environmental, 2009, 87, 30-36. | 10.8 | 84 |
| 461 | Photoeletrochemical generation of hydrogen over carbon-doped TiO2 photoanode. Applied Catalysis B: Environmental, 2009, 92, 41-49. | 10.8 | 55 |
| 462 | Catalytic Ozonation of Selected Pharmaceuticals over Mesoporous Alumina-Supported Manganese Oxide. Environmental Science & Technology, 2009, 43, 2525-2529. | 4.6 | 203 |
| 463 | The influence of Cu(II) on the decay of monochloramine. Chemosphere, 2009, 74, 181-186. | 4.2 | 10 |
| 464 | Electrochemical process combined with UV light irradiation for synergistic degradation of ammonia in chloride-containing solutions. Water Research, 2009, 43, 1432-1440. | 5.3 | 125 |
| 465 | Degradation of selected pharmaceuticals in aqueous solution with UV and UV/H2O2. Water Research, 2009, 43, 1766-1774. | 5.3 | 288 |
| 466 | Indirect Photodegradation of Amine Drugs in Aqueous Solution under Simulated Sunlight. Environmental Science & Technology, 2009, 43, 2760-2765. | 4.6 | 195 |
| 467 | Effect of Aluminum Speciation and Structure Characterization on Preferential Removal of Disinfection Byproduct Precursors by Aluminum Hydroxide Coagulation. Environmental Science & Technology, 2009, 43, 5067-5072. | 4.6 | 76 |
| 468 | Natural organic matter removal by coagulation: effect of kinetics and hydraulic power. Water Science and Technology: Water Supply, 2009, 9, 21-30. | 1.0 | 12 |

| # | Article | IF | CITATIONS |
|-----|---|------|-----------|
| 469 | Species transformation and structure variation of fulvic acid during ozonation. Science in China Series B: Chemistry, 2008, 51, 373-378. | 0.8 | 5 |
| 470 | Proportion of bromo-DBPs in total DBPs during reclaimed-water chlorination and its related influencing factors. Science in China Series B: Chemistry, 2008, 51, 1000-1008. | 0.8 | 8 |
| 471 | Formation and distribution of disinfection by-products during chlorine disinfection in the presence of bromide ion. Science Bulletin, 2008, 53, 2717-2723. | 4.3 | 9 |
| 472 | Photodegradation of tetracycline and formation of reactive oxygen species in aqueous tetracycline solution under simulated sunlight irradiation. Journal of Photochemistry and Photobiology A: Chemistry, 2008, 197, 81-87. | 2.0 | 249 |
| 473 | The formation and distribution of haloacetic acids in copper pipe during chlorination. Journal of Hazardous Materials, 2008, 152, 250-258. | 6.5 | 24 |
| 474 | Cyanobacteria and their toxins in Guanting Reservoir of Beijing, China. Journal of Hazardous Materials, 2008, 153, 470-477. | 6.5 | 52 |
| 475 | Efficient photodegradation of Acid Red B by immobilized ferrocene in the presence of UVA and H2O2. Journal of Hazardous Materials, 2008, 154, 146-152. | 6.5 | 55 |
| 476 | Mineralization of an azo dye Acid Red 14 by photoelectro-Fenton process using an activated carbon fiber cathode. Applied Catalysis B: Environmental, 2008, 84, 393-399. | 10.8 | 154 |
| 477 | Microwave electrodeless lamp assisted catalytic degradation of X-GRL with manganese dioxides: Adsorption and manganese(IV) reductive dissolution effects. Catalysis Today, 2008, 139, 119-124. | 2.2 | 12 |
| 478 | An efficient electron transfer at the Fe0/iron oxide interface for the photoassisted degradation of pollutants with H2O2. Applied Catalysis B: Environmental, 2008, 82, 151-156. | 10.8 | 31 |
| 479 | Enhanced degradation of 2,4-dinitrotoluene by ozonation in the presence of manganese(II) and oxalic acid. Journal of Molecular Catalysis A, 2008, 286, 149-155. | 4.8 | 68 |
| 480 | Characterization and Reactivity of MnO _{<i>x</i>} Supported on Mesoporous Zirconia for Herbicide 2,4-D Mineralization with Ozone. Environmental Science & Technology, 2008, 42, 3363-3368. | 4.6 | 118 |
| 481 | Research progress of novel adsorption processes in water purification: A review. Journal of Environmental Sciences, 2008, 20, 1-13. | 3.2 | 369 |
| 482 | Nitrobenzene biodegradation ability of microbial communities in water and sediments along the Songhua River after a nitrobenzene pollution event. Journal of Environmental Sciences, 2008, 20, 778-786. | 3.2 | 42 |
| 483 | Phototransformation of nitrobenzene in the Songhua River: Kinetics and photoproduct analysis. Journal of Environmental Sciences, 2008, 20, 787-795. | 3.2 | 20 |
| 484 | Preparation and visible-light activity of silver vanadate for the degradation of pollutants. Materials Research Bulletin, 2008, 43, 2986-2997. | 2.7 | 64 |
| 485 | Catalytic Ozonation of Herbicide 2,4-D over Cobalt Oxide Supported on Mesoporous Zirconia. Journal of Physical Chemistry C, 2008, 112, 5978-5983. | 1.5 | 70 |
| 486 | Enhanced coagulation for high alkalinity and micro-polluted water: The third way through coagulant optimization. Water Research, 2008, 42, 2278-2286. | 5.3 | 141 |

| # | Article | IF | CITATIONS |
|-----|---|-----|-----------|
| 487 | Mechanism of natural organic matter removal by polyaluminum chloride: Effect of coagulant particle size and hydrolysis kinetics. Water Research, 2008, 42, 3361-3370. | 5.3 | 220 |
| 488 | Relationship of energy charge and toxin content of Microcystis aeruginosa in nitrogen-limited or phosphorous-limited cultures. Toxicon, 2008, 51, 649-658. | 0.8 | 40 |
| 489 | Effect of preozonation on the characteristic transformation of fulvic acid and its subsequent trichloromethane formation potential: Presence or absence of bicarbonate. Chemosphere, 2008, 71, 1639-1645. | 4.2 | 18 |
| 490 | Effect of manganese ion on the mineralization of 2,4-dichlorophenol by ozone. Chemosphere, 2008, 72, 1006-1012. | 4.2 | 33 |
| 491 | Design of BDD-TiO ₂ Hybrid Electrode with Pâ^'N Function for Photoelectrocatalytic Degradation of Organic Contaminants. Environmental Science & Technology, 2008, 42, 4934-4939. | 4.6 | 74 |
| 492 | Bactericidal Activity of a Ce-Promoted Ag/AlPO4 Catalyst Using Molecular Oxygen in Water. Environmental Science & Technology, 2008, 42, 1699-1704. | 4.6 | 22 |
| 493 | Role of Aluminum Speciation in the Removal of Disinfection Byproduct Precursors by a Coagulation Process. Environmental Science & amp; Technology, 2008, 42, 5752-5758. | 4.6 | 123 |
| 494 | Electrochemical Degradation of Cyanobacterial Toxin Microcystin-LR Using Ti/RuO ₂ Electrodes in a Continuous Tubular Reactor. Environmental Engineering Science, 2008, 25, 635-642. | 0.8 | 16 |
| 495 | Preparation and evaluation of a novel Fe–Mn binary oxide adsorbent for effective arsenite removal. Water Research, 2007, 41, 1921-1928. | 5.3 | 538 |
| 496 | A biomimetic absorbent for removal of trace level persistent organic pollutants from water. Environmental Pollution, 2007, 147, 337-342. | 3.7 | 16 |
| 497 | CuFe2O4/activated carbon composite: A novel magnetic adsorbent for the removal of acid orange II and catalytic regeneration. Chemosphere, 2007, 68, 1058-1066. | 4.2 | 270 |
| 498 | Effects of copper(II) and copper oxides on THMs formation in copper pipe. Chemosphere, 2007, 68, 2153-2160. | 4.2 | 36 |
| 499 | Photoelectrocatalytic Degradation of Triazine-Containing Azo Dyes at γ-Bi ₂ MoO ₆ Film Electrode under Visible Light Irradiation (λ > 420 Nm). Environmental Science & Technology, 2007, 41, 6802-6807. | 4.6 | 118 |
| 500 | Photoassisted Degradation of Azodyes over FeOxH2x-3/FeO in the Presence of H2O2 at Neutral pH Values. Environmental Science & Technology, 2007, 41, 4715-4719. | 4.6 | 47 |
| 501 | Bactericidal Mechanism of Ag/Al ₂ O ₃ against <i>Escherichia coli</i> . Langmuir, 2007, 23, 11197-11199. | 1.6 | 60 |
| 502 | Photocatalytic Degradation of Pathogenic Bacteria with AgI/TiO2under Visible Light Irradiation. Langmuir, 2007, 23, 4982-4987. | 1.6 | 217 |
| 503 | Alkalinity effect of coagulation with polyaluminum chlorides: Role of electrostatic patch. Colloids and Surfaces A: Physicochemical and Engineering Aspects, 2007, 294, 163-173. | 2.3 | 97 |
| 504 | Adsorption and reduction of nitrate in water on hydrotalcite-supported Pd-Cu catalyst. Catalysis Today, 2007, 126, 476-482. | 2.2 | 38 |

| # | Article | IF | CITATIONS |
|-----|--|------|-----------|
| 505 | Effect of liquid property on adsorption and catalytic reduction of nitrate over hydrotalcite-supported Pd-Cu catalyst. Journal of Molecular Catalysis A, 2007, 272, 31-37. | 4.8 | 48 |
| 506 | Removal of dieldrin from aqueous solution by a novel triolein-embedded composite adsorbent. Journal of Hazardous Materials, 2007, 141, 61-69. | 6.5 | 36 |
| 507 | Degradation of azo dye Acid Orange 7 in water by Fe0/granular activated carbon system in the presence of ultrasound. Journal of Hazardous Materials, 2007, 144, 180-186. | 6.5 | 174 |
| 508 | Catalytic sterilization of Escherichia coli K 12 on Ag/Al2O3 surface. Journal of Inorganic Biochemistry, 2007, 101, 817-823. | 1.5 | 32 |
| 509 | Relative importance of hydrolyzed Al(III) species (Ala, Alb, and Alc) during coagulation with polyaluminum chloride: A case study with the typical micro-polluted source waters. Journal of Colloid and Interface Science, 2007, 316, 482-489. | 5.0 | 143 |
| 510 | Efficient destruction of pathogenic bacteria with AgBr/TiO2 under visible light irradiation. Applied Catalysis B: Environmental, 2007, 73, 354-360. | 10.8 | 86 |
| 511 | Efficient destruction of bacteria with Ti(IV) and antibacterial ions in co-substituted hydroxyapatite films. Applied Catalysis B: Environmental, 2007, 73, 345-353. | 10.8 | 65 |
| 512 | Silicate Hindering In Situ Formed Ferric Hydroxide Precipitation: Inhibiting Arsenic Removal from Water. Environmental Engineering Science, 2007, 24, 707-715. | 0.8 | 20 |
| 513 | Formation and transformation of Al13 from freshly formed precipitate in partially neutralized Al(III) solution. Journal of Sol-Gel Science and Technology, 2007, 41, 257-265. | 1.1 | 8 |
| 514 | Development and application of innovative technologies for drinking water quality assurance in China. Frontiers of Environmental Science and Engineering in China, 2007, 1, 257-269. | 0.8 | 13 |
| 515 | Coagulation Behavior of Aluminum Salts in Eutrophic Water:Â Significance of Al13Species and pH Control. Environmental Science & Technology, 2006, 40, 325-331. | 4.6 | 256 |
| 516 | Ag/AgBr/TiO2Visible Light Photocatalyst for Destruction of Azodyes and Bacteria. Journal of Physical Chemistry B, 2006, 110, 4066-4072. | 1.2 | 552 |
| 517 | Visible-Light-Induced Photocatalytic Degradation of Azodyes in Aqueous Agl/TiO2Dispersion. Environmental Science & Technology, 2006, 40, 7903-7907. | 4.6 | 180 |
| 518 | Efficient Destruction of Pathogenic Bacteria with NiO/SrBi2O4under Visible Light Irradiation. Environmental Science & Technology, 2006, 40, 5508-5513. | 4.6 | 81 |
| 519 | Electrochemically assisted photocatalytic degradation of Acid Orange 7 with β-PbO2 electrodes modified by TiO2. Water Research, 2006, 40, 213-220. | 5.3 | 100 |
| 520 | The electrocatalytic reduction of nitrate in water on Pd/Sn-modified activated carbon fiber electrode. Water Research, 2006, 40, 1224-1232. | 5.3 | 103 |
| 521 | Enhanced coagulation in a typical North-China water treatment plant. Water Research, 2006, 40, 3621-3627. | 5.3 | 83 |
| 522 | Electrocatalytic Reduction of Nitrate in Water with a Palladium-Modified Copper Electrode. Water Environment Research, 2006, 78, 724-729. | 1.3 | 19 |

Јіиниі Qu

| # | Article | IF | CITATIONS |
|-----|---|------|-----------|
| 523 | Fe(VI)-assisted photocatalytic degradating of microcystin-LR using titanium dioxide. Journal of Photochemistry and Photobiology A: Chemistry, 2006, 178, 106-111. | 2.0 | 36 |
| 524 | Microwave electrodeless lamp photolytic degradation of acid orange 7. Journal of Photochemistry and Photobiology A: Chemistry, 2006, 184, 26-33. | 2.0 | 47 |
| 525 | Oxidative decomposition of azo dye C.I. Acid Orange 7 (AO7) under microwave electrodeless lamp irradiation in the presence of H2O2. Journal of Hazardous Materials, 2006, 134, 183-189. | 6.5 | 60 |
| 526 | Electrochemically assisted photocatalytic degradation of Orange II: Influence of initial pH values. Journal of Molecular Catalysis A, 2006, 259, 238-244. | 4.8 | 96 |
| 527 | Hydrotalcite-supported Pd-Cu catalyst for nitrate adsorption and reduction from water. Science Bulletin, 2006, 51, 1431-1438. | 4.3 | 9 |
| 528 | Coagulation properties of an electrochemically prepared polyaluminum chloride containing active chlorine. Science Bulletin, 2006, 51, 1955-1960. | 1.7 | 2 |
| 529 | Photocatalytic decomposition of acetaldehyde and Escherichia coli using NiO/SrBi2O4 under visible light irradiation. Applied Catalysis B: Environmental, 2006, 69, 17-23. | 10.8 | 55 |
| 530 | Removal of a type of endocrine disruptors—di-n-butyl phthalate from water by ozonation. Journal of Environmental Sciences, 2006, 18, 845-851. | 3.2 | 17 |
| 531 | Pd-Cu/水滑石å₅∕附å,¬åŒ–æ°¢è;~原水ä,çš,,ç¡é…,æ¹. Chinese Science Bulletin, 2006, 51, 786-791. | 0.4 | 1 |
| 532 | Coagulation behavior of aluminum salts in eutrophic water: significance of Al13 species and pH control. Environmental Science & Technology, 2006, 40, 325-31. | 4.6 | 11 |
| 533 | Mineralization of an azo dye Acid Red 14 by electro-Fenton's reagent using an activated carbon fiber cathode. Dyes and Pigments, 2005, 65, 227-233. | 2.0 | 286 |
| 534 | Preparation and characteristic of triolein-embedded composite sorbents for water purification. Separation and Purification Technology, 2005, 44, 37-43. | 3.9 | 13 |
| 535 | Photoelectrochemical synergetic degradation of Acid Orange II with TiO2 modified Î ² -PbO2 electrode. Science Bulletin, 2005, 50, 1185-1190. | 1.7 | 11 |
| 536 | Inactivation ofMicrocystis aeruginosaby Continuous Electrochemical Cycling Process in Tube Using Ti/RuO2Electrodes. Environmental Science & Technology, 2005, 39, 4633-4639. | 4.6 | 97 |
| 537 | Magnetic powder MnO–Fe2O3 composite—a novel material for the removal of azo-dye from water. Water Research, 2005, 39, 630-638. | 5.3 | 232 |
| 538 | Removal of azo-dye Acid Red B (ARB) by adsorption and catalytic combustion using magnetic CuFe2O4 powder. Applied Catalysis B: Environmental, 2004, 48, 49-56. | 10.8 | 146 |
| 539 | Ozonation of alachlor catalyzed by Cu/Al2O3 in water. Catalysis Today, 2004, 90, 291-296. | 2.2 | 77 |
| 540 | Optimum conditions for Al13 polymer formation in PACl preparation by electrolysis process. Chemosphere, 2004, 55, 51-56. | 4.2 | 27 |

| # | Article | IF | CITATIONS |
|-----|--|-----|-----------|
| 541 | Novel synergic combinatorial photoelectrochemical technology for degradation of trace of 2-chlorophenol in drinking water. Science Bulletin, 2003, 48, 751-757. | 1.7 | 1 |
| 542 | Degradation of azo dye acid red B on manganese dioxide in the absence and presence of ultrasonic irradiation. Journal of Hazardous Materials, 2003, 100, 197-207. | 6.5 | 89 |
| 543 | Combined bioelectrochemical and sulfur autotrophic denitrification for drinking water treatment. Water Research, 2003, 37, 3767-3775. | 5.3 | 74 |
| 544 | Comparison of Two Combined Bioelectrochemical and Sulfur Autotrophic Denitrification Processes for Drinking Water Treatment. Journal of Environmental Science and Health - Part A Toxic/Hazardous Substances and Environmental Engineering, 2003, 38, 1269-1284. | 0.9 | 5 |
| 545 | Fluorimetric Determination of Arsenite and Arsenate in Water Using Fluorescein and Iodine. International Journal of Environmental Analytical Chemistry, 2002, 82, 31-36. | 1.8 | 8 |
| 546 | DENITRIFICATION OF DRINKING WATER BY A COMBINED PROCESS OF HETEROTROPHICATION AND ELECTROCHEMICAL AUTOTROPHICATION. Journal of Environmental Science and Health - Part A Toxic/Hazardous Substances and Environmental Engineering, 2002, 37, 651-665. | 0.9 | 1 |
| 547 | The electrochemical production of highly effective polyaluminum chloride. Water Research, 1999, 33, 807-813. | 5.3 | 53 |